

CHAPTER TWENTY-ONE

Eastern Hemisphere

21.1	The Tectonic Evolution of the European Alps and Forelands—An essay by Stefan M. Schmid	510	21.3	Tectonics of the Altai: An Example of a Turkic-type Orogen—An essay by A. M. Clal Őengr and Boris A. Natal'in	535
21.2	The Tibetan Plateau and Surrounding Regions—An essay by Leigh H. Royden and B. Clark Burchfiel	525	21.4	The Tasman Orogenic Belt, Eastern Australia: An Example of Paleozoic Tectonic Accretion—An essay by David R. Gray and David A. Foster	547

21.1 THE TECTONIC EVOLUTION OF THE EUROPEAN ALPS AND FORELANDS—An essay by Stefan M. Schmid¹

21.1.1 Introduction	510	21.1.6 Evolution of the Alpine System and Its Forelands in Time Slices	517
21.1.2 The Major Tectonic Units of the European Alps	510	21.1.7 Recent Movements in the Upper Rhine Graben	522
21.1.3 The Major Paleogeographic Units of the Alps	512	21.1.8 Closing Remarks	523
21.1.4 Three Alpine Transects and Their Deep Structure	514	Additional reading	524
21.1.5 Inferences Concerning Rheologic Behavior	517		

21.1.1 Introduction

The **European Alps**, located in south-central Europe, record the closure of several ocean basins in the Mediterranean region during convergence between the African and European Plates. This contribution gives a short overview of the overall architecture of the western and central Alps of Europe and their forelands (Po plain and northern foreland), based mostly on three recent geophysical-geological transects, the locations of which are given in Figure 21.1.1. The evolution of the Alpine system is discussed in time slices, starting with Cretaceous orogeny and ending with evidence for very recent movements in the area of the Rhine Graben. Some aspects of neotectonics and earthquake hazard will be addressed as well.

21.1.2 The Major Tectonic Units of the European Alps

The simplified sketch map of the Alps in Figure 21.1.1 highlights the transition from the central to the western Alps, which will be discussed along three major transects. The Insubric line marks the northern and western boundary of the southern Alps. The southern Alps are characterized by a dominantly south-verging fold-and-thrust belt whose southern tip is stratigraphically sealed by the Messinian (7 Ma) unconformity below

the Po plain. At the base of this very young (Miocene) foreland prism we find the Adriatic middle and lower crust, including the Adriatic mantle, from which 10- to 15-km thick slices, consisting of basement and its Mesozoic sedimentary cover have been detached (see Figure 21.1.3c). This style of deformation points to the availability of a potential décollement (detachment) horizon within the granitic upper crust at a depth interval of 10–15 km, corresponding to temperatures in the range of 250°–375°C (assuming a gradient of 25°C/km). This depth probably corresponds to the brittle–plastic transition within granitic crust. The transition is due to the onset of crystal plasticity in quartz (at about 270°C), and/or reaction-enhanced ductility due to breakdown reactions of feldspar at about 250°C. Before this postcollisional Miocene shortening, during Paleogene plate convergence and collision, the lithosphere of the present-day southern Alps (the Adriatic Plate) formed the upper plate, under which the Penninic Valais and Piemont-Liguria Oceans, an intervening microcontinent (Briançonnais), and the European continental margin were subducted (see Figure 21.1.5a–c). Figure 21.1.1 also depicts the outlines of the Ivrea geophysical body, which represents the western edge of the Adriatic Plate. The Ivrea zone, a belt of south Alpine lower-crustal rocks, is the surface expression of the Ivrea geophysical body. Because this lower crust has been exhumed to moderate depth (corresponding to less than 300°C) during Mesozoic rifting, it represents a particularly rigid part of the south Alpine basement at the west-northwest front of the Adriatic indenter.

¹Department of Earth Sciences, Basel, Switzerland.

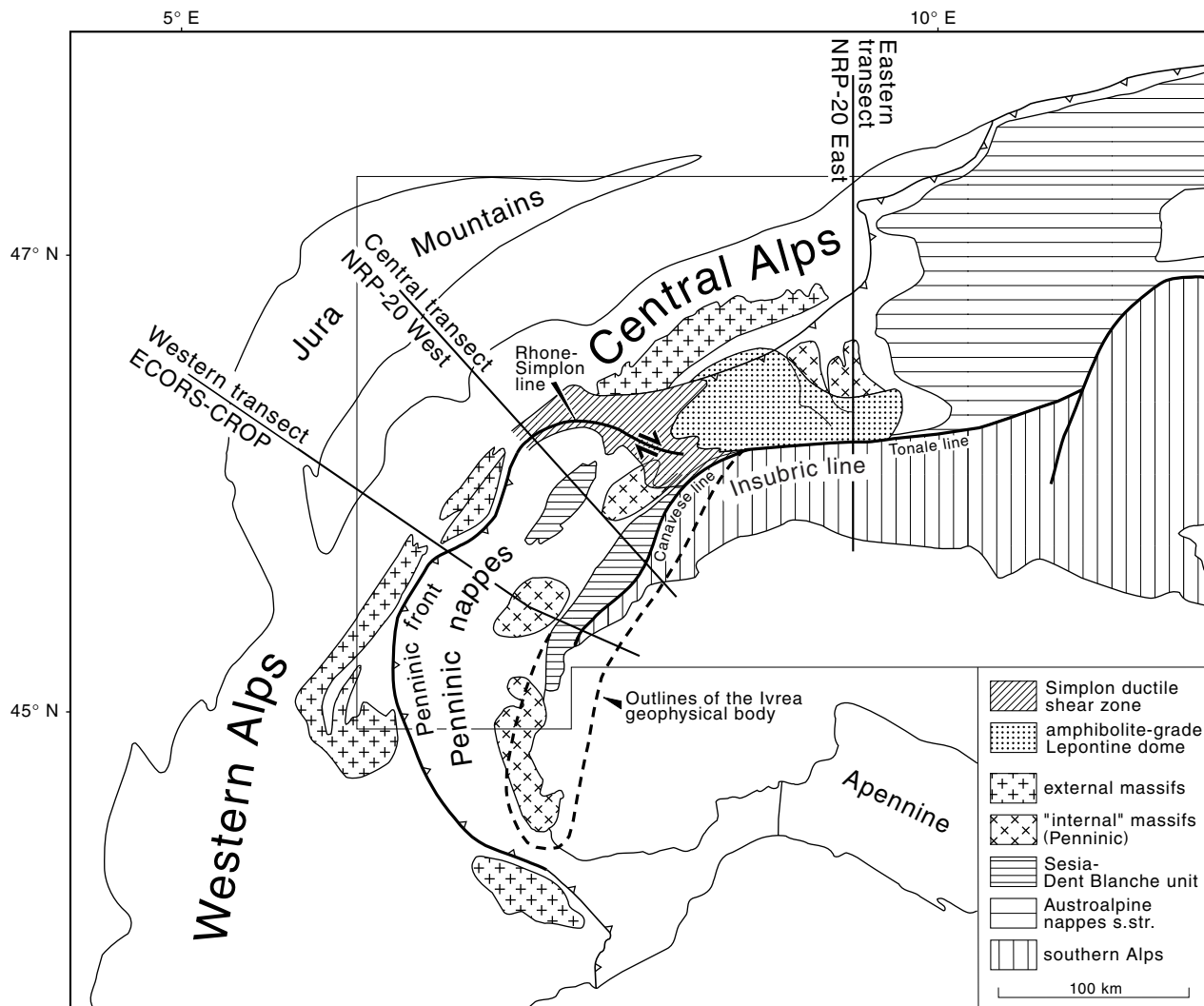


FIGURE 21.1.1 Sketch map of the Alps, indicating locations of the three geophysical-geological transects depicted in Figure 21.1.3.

Most of the roughly 100-km Oligo-Miocene dextral strike-slip along the east-west striking eastern branch of the Insubric line (the Tonale line) has been taken up by dextral strike-slip movements along the Simplon ductile shear zone and the Rhone-Simplon line. Hence, from Oligocene to probably recent times, the western Alps are kinematically part of the west-northwest moving Adriatic indenter, causing west-northwest directed thrusting along the Penninic front of the western Alps and within the Dauphinois foreland. The Rhone-Simplon line continues to act as a major discontinuity up to the present day, both in terms of seismic activity and in the character of the stress regime. During the latest stages of orogeny, this west-

northwest directed indenting by the Adriatic Plate possibly migrated further into the foreland, also affecting the western Molasse Basin and causing arcuate folding in the Jura Mountains.

The central Alps are characterized by ongoing north-south shortening that occurred during the Oligocene-Miocene, coeval with west-northwest to east-southeast shortening in the western Alps. These diverging transport directions necessitate an orogen-parallel extension, the effect of which is best documented by the Simplon normal fault and the exhumed amphibolite-grade Lepontine dome in its footwall. Oligo-Miocene exhumation of the Lepontine dome is the result of the combined effect of orogen-parallel

extension, backthrusting along the Insubric line, and fast erosion.

The units north of the Insubric line consist of the Austroalpine nappes outcropping in eastern Switzerland and extending into Austria. Although paleogeographic provenance of these units is similar to that of the southern Alps, they consist of completely rootless slivers of basement and cover that have been detached (or delaminated) from their lithosphere during Cretaceous orogeny. These nappes have been stacked towards the west-northwest and their former (Cretaceous) tectonic front runs almost perpendicular to the present-day Alps in eastern Switzerland (Grisons). The Sesia-Dent Blanche unit of the western Alps underwent an Alpine tectono-metamorphic history that is different from that of the Austroalpine nappes and the southern Alps (subducted near the Cretaceous-Tertiary boundary). However, its pre-Alpine basement exhibits close similarities to that of the southern Alps.

The Penninic units are of extremely heterogeneous paleogeographic provenance, containing remnants of oceanic lithosphere, a continental fragment referred to as Briançonnais, as well as basement of the European margin. Deformation is penetrative and polyphase, and most of the Penninic units are overprinted by metamorphism, except for the Préalpes Romandes that have been detached and transported towards the northern foreland during the Eocene.

The Helvetic nappes have been detached from their former crystalline basement, which must be looked for in the lowermost Penninic nappes. The units still attached to the European lithosphere consist of the external massifs and their cover, slightly detached from the lower crust during the Miocene, when deformation started to migrate into the foreland, eventually displacing the western Molasse Basin and the Jura Mountains by up to 30 km from the Serravallian (12 Ma) onwards. The southern Rhine Graben represents an Eocene-Oligocene continental rift, kinematically linked to the Bresse Graben situated west of the Jura Mountains and ultimately to the opening of the western Mediterranean Basin (but not to the Alps). The geometry of Oligocene extensional faulting exerts a profound influence on Miocene to recent movements in the Jura Mountains and their northern margin in the southern Rhine Graben.

21.1.3 The Major Paleogeographic Units of the Alps

The major paleogeographic units of the Alps are shown in Figure 21.1.2. Many of the units are only preserved as extremely thin slivers that were detached

from the subducting lithosphere and that accreted as slices (so-called nappes) to the upper plate (Austroalpine and south Alpine units). A description of the main units follows.

European margin: This consists of external massifs and their cover (extending northward underneath the Molasse Basin) and Helvetic cover nappes, whose crystalline substratum lies within the deepest part of the Lepontine dome (lowermost “Penninic” nappes). Note that the European-derived basement can be traced southward almost to the Insubric line. This demonstrates very substantial exhumation of formerly subducted and newly accreted European lithosphere during the formation of the Lepontine dome. Its later exhumation is due to a combined effect of retroflow (backfolding and backthrusting along the Insubric line) and unroofing by orogen-parallel extension and erosion during the postcollisional stages of orogeny. Some of these units also underwent Tertiary eclogitization.

Valais Ocean: The remnants of this ocean predominantly consist of Cretaceous Bündnerschiefer, grading into Tertiary flysch and at least partly deposited onto oceanic lithosphere. Eclogitic mafic rocks are preserved in the Versoyen of the western Alps, while blueschists and other low temperature-high pressure rocks are preserved in the Engadine window. The Valais Ocean opened near the Jurassic-Cretaceous boundary; its remnants presently define a northern Alpine suture zone that closed during the Late Eocene.

Briançonnais microcontinent: This microcontinent was attached to Iberia (Spain) and formed the northern passive continental margin of the Jurassic Piemont-Liguria Ocean, before it broke off the European margin in conjunction with the opening of the Valais Ocean. The Mesozoic cover of the Briançonnais microcontinent largely consists of platform sediments with frequent stratigraphic gaps (“mid-Penninic swell”). Its basement is preserved in the form of the Tambo-Suretta, Maggia, and Bernhard–M. Rosa nappes in the eastern, central, and western Penninic realm, respectively. Detached cover nappes form a substantial part of the Préalpes Romandes.

Piemont-Liguria Basin: This consists of oceanic lithosphere formed during the Middle Jurassic to Early Cretaceous and is characterized by a classic Alpine ophiolite suite. Seafloor spreading was followed by the deposition of radiolarites and aptycha limestones. During the Cretaceous, the deposition

Paleogeographic Units in the Alps

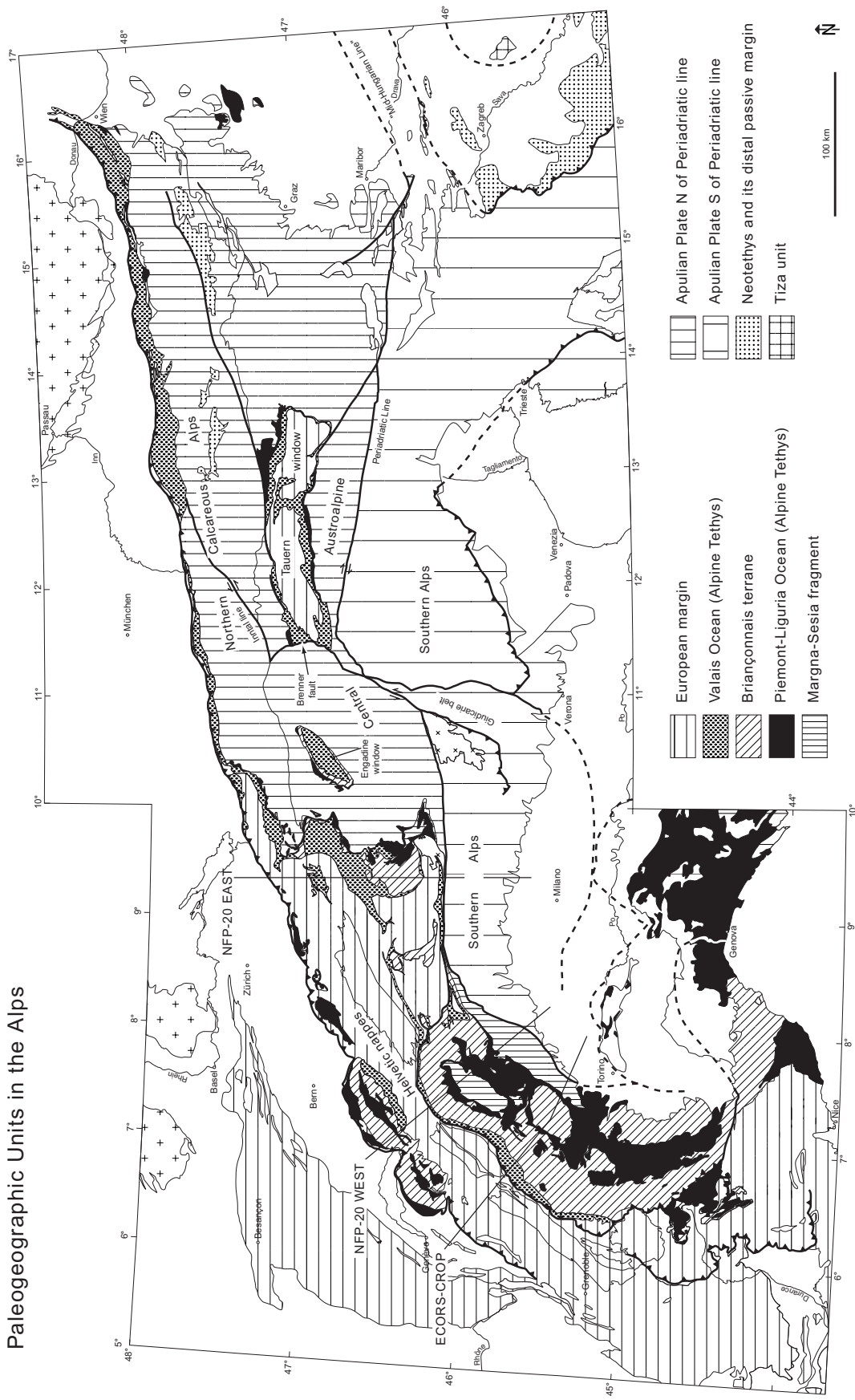


FIGURE 21.1.2 Paleogeographic map of the Alps, indicating the present-day position of the major paleogeographic units of the Alps.

of trench deposits (Avers Bündnerschiefer of Eastern Switzerland and schistes lustrées of western Switzerland) indicates that the southern (Apulian) margin of this basin had been converted into an active margin. In eastern Switzerland, the Piemont-Liguria units (Arosa and Platta unit) were involved in Cretaceous orogenic activity. However, the Piemont-Liguria Ocean did not completely close before the onset of orogeny in the Tertiary.

Margna-Sesia fragment: A small fragment of the Apulian margin, rifted off Apulia during the opening of the Piemont-Liguria Ocean and was later incorporated into the accretionary wedge along the active northern margin of Apulia.

Apulian margin: North of the Insubric line, this southern margin is only preserved in the form of rootless basement and cover slices (Austroalpine nappes). South of the Insubric line it corresponds to the southern Alps and their lithospheric substratum, the Adriatic Plate (which is part of the larger “Apulian” Plate).

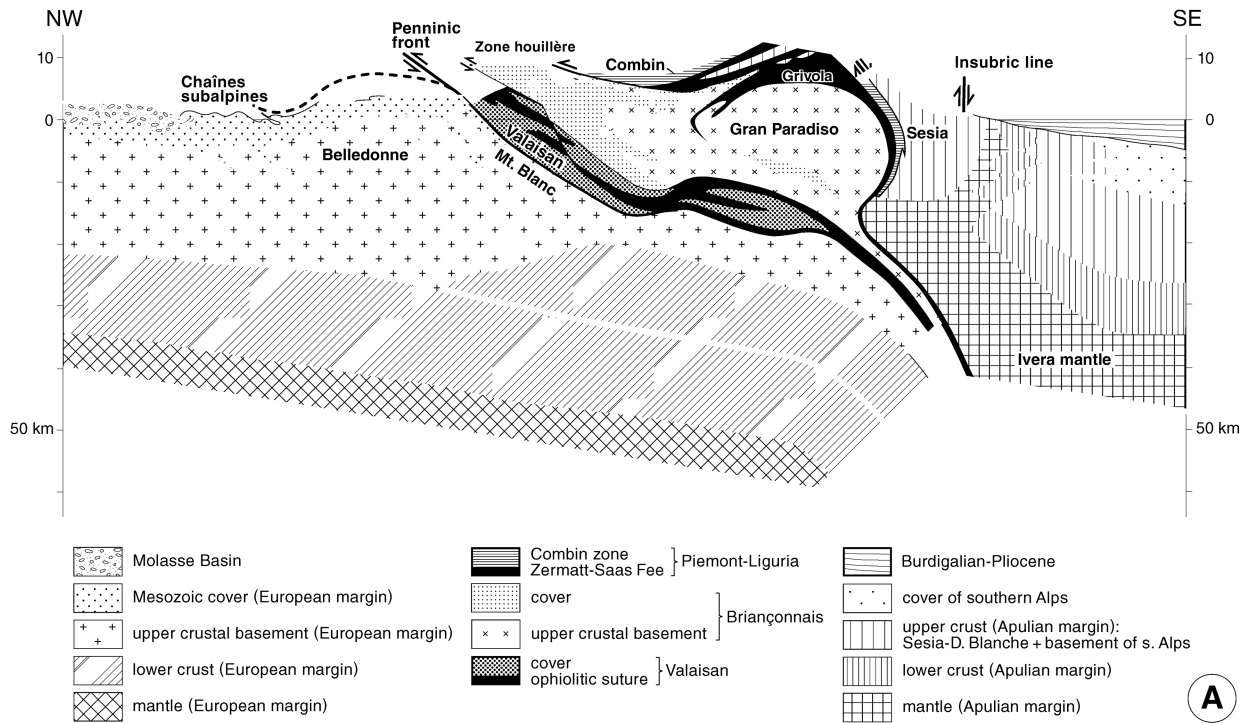
Neotethys Ocean: This is a third oceanic domain, associated with the so-called Meliata-Hallstatt ocean, formed during the Triassic. In the Alps, only the distal passive margin is preserved (Hallstatt), while ophiolitic remnants (Meliata) are found in the Dinarides and the western Carpathians. This ocean is of significance mostly for the role it plays in understanding Cretaceous (or Eoalpine) orogeny.

21.1.4 Three Alpine Transects and Their Deep Structure

The major features common to all three transects, schematically sketched in Figure 21.1.3, are (1) ESE–S-directed subduction of the European lithosphere, (2) a gap between European and Adriatic Moho, and (3) the presence of wedge-shaped bodies of lower crust, largely decoupled from the piling up and refolding of thin flakes of upper-crustal material (the Alpine nappes). However, there are substantial differences in the geometry and kinematic evolution of the eastern transect (Figure 21.1.3c) as compared to the western and central transects (Figure 21.1.3a and b, respectively). Based on a study of these sections, the following observations are made:

- In the eastern (NRP-20 East) transect (Figure 21.1.3c) the Adriatic Moho descends northward and toward its contact with the lower (European) crust, while in the central and western transects (Figure 21.1.3a and b) this same Adriatic Moho rises toward the surface when approaching the contact zone with the European lithosphere. This contrast is also expressed in the surface geology. In the eastern transect, the southern Alps form an impressive south-vergent foreland fold-and-thrust belt (“retrowedge”) riding above the Adriatic lower crust, while this same Adriatic lower crust is exposed in the Ivrea zone, situated at the Southeast end of the central and western transects. The Ivrea zone and Ivrea geophysical body wedge out eastward and do not extend into the area covered by the eastern transect.
- In the eastern (NRP-20 East) transect, a wedge of Adriatic lower crust is found above European lower crust and below European upper crust at its northern end. This slice of Adriatic lower crust was wedged into the European lithosphere during the Miocene, splitting apart along the boundary between the upper and lower crust. For the western (ECORS-CROP) and central (NRP-20 West) transects a geometrically different process of wedging is inferred. In these latter two cases, however, the lower crustal wedge is interpreted to be derived from the European lithosphere. Hence the wedges of lower crust seen in the eastern (Figure 21.1.3c), and the western and central transects (Figure 21.1.3a and b), respectively, are of different origin and, thus, cannot be laterally connected. This implies that the Adriatic lower crust descends below the Penninic nappe stack in the eastern profile, while it rises to the surface in the western transect, independently supports the conclusion that the two lower crustal wedges are not laterally connected.
- In the area immediately north of the Insubric line, the eastern transect (NRP-20 East) exhibits substantial backthrusting and backfolding of all the Penninic nappes, including the Valais suture zone. This was associated with exhumation of the amphibolite-grade Lepontine dome and the deep-seated Bergell Massif. In the western transect (ECORS-CROP), however, backthrusting does not affect the Valais suture zone and appears to be restricted to the units above this suture (within the Briançonnais upper crust). Note that Barrovian-type amphibolite-grade

ECORS-CROP



NFP-20 WEST

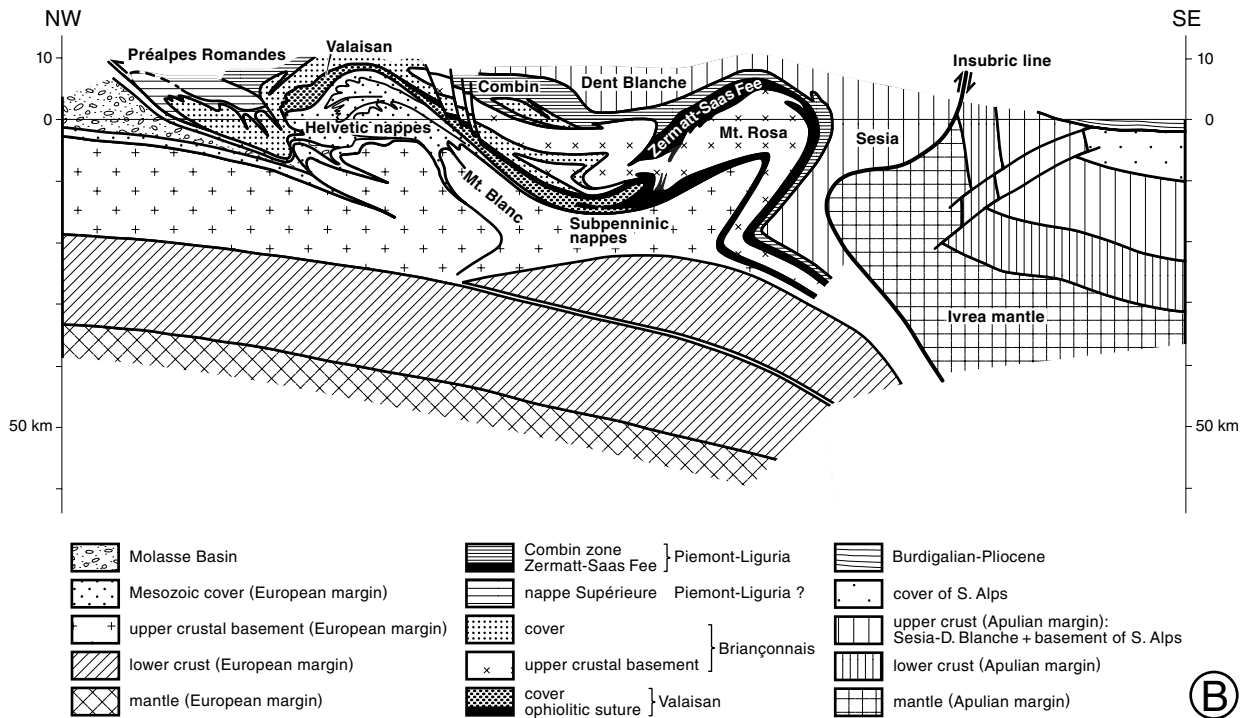


FIGURE 21.1.3 Three schematic geophysical-geological cross sections through the western and central Alps (profile traces indicated in Figure 21.1.1). Superimposed circles mark earthquake foci for the 1980–1995 time period. These foci are projected into the sections from within a 30-km traverse.

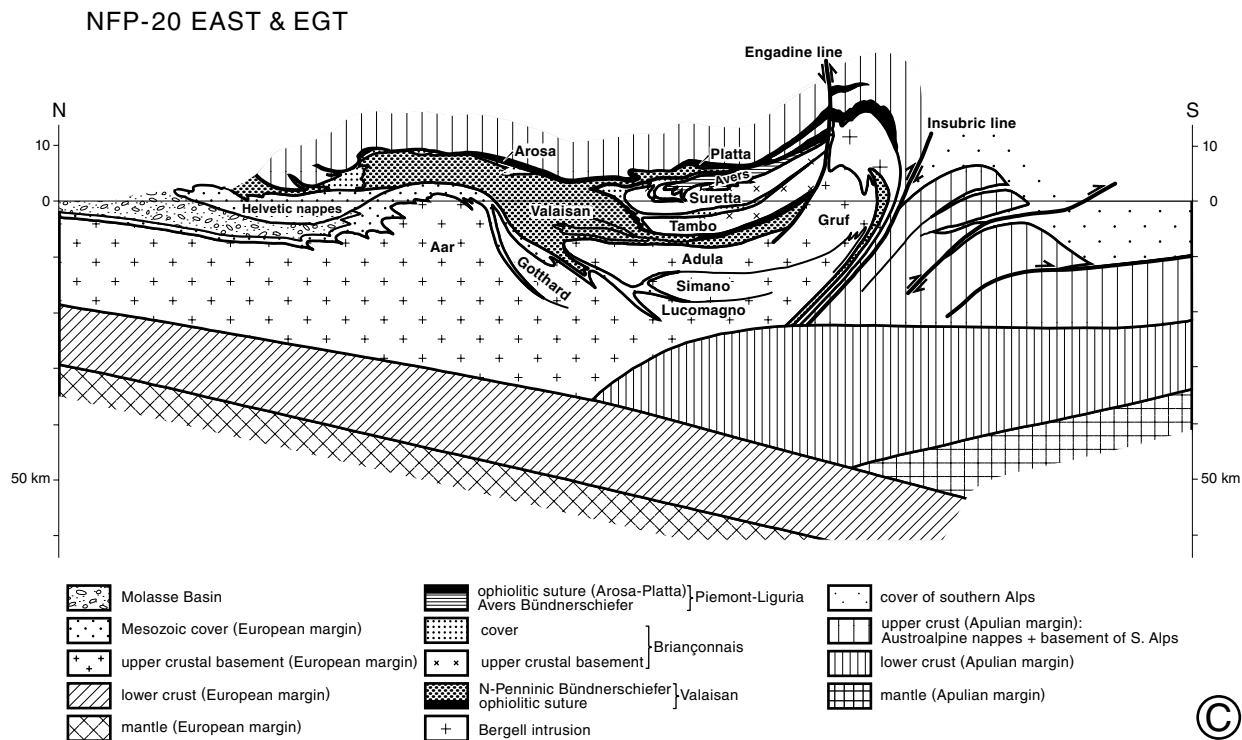


FIGURE 21.1.3 (Continued)

rocks have not been exhumed to the surface in the western transect, where the Insubric line only exhibits minor vertical offset.

- The orogenic lid of the Austroalpine nappes, under which Penninic and Helvetic nappes were accreted in the eastern transect, is absent in the western and central transects.
- Accurately located earthquakes, when orthogonally projected over a maximum distance of 30-km onto the transects of Figure 21.1.3 (see Schmid and Kissling, 2000), show significant differences in the depth of seismogenic regions. The maximum depth of earthquakes is situated near the Moho in the northern and southern forelands along the eastern traverse (Figure 21.1.3c). Beneath the Penninic units (i.e., within the Lepontine metamorphic dome), they are restricted to the thickened upper crust. Also note that the Adriatic lower crustal wedge is quiescent. Coincidence of the lower limit of seismicity with predicted isotherms based on thermal modeling suggests that the 500°C isotherm controls the cataclastic–plastic transition. Quiescence within the Adriatic lower crustal wedge further suggests that, in the case of the central Alps, stress transmission between the European and Adriatic lithosphere is largely restricted to upper crustal levels. In contrast, the earthquake distribution along

the western and, to a lesser degree, along the central transects exhibits a wide, east-dipping corridor of foci affecting the entire transect, including the allochthonous European lower crust (Figure 21.1.3a and b). Thus, mechanical coupling and stress transmission between the Adriatic microplate and the European lithosphere occur along a deep-reaching seismogenic zone. This indicates a contrasting (with respect to the eastern transect) thermal regime, primarily because of the following substantial differences in kinematic evolution. First, oblique convergence and collision in the western Alps before 35 Ma must have led to a significantly smaller volume of accreted radiogenic upper crustal rocks, as compared to the central Alps, the latter being characterized by head-on convergence and collision. Secondly, double-verging displacements of the central and western Alps after 35 Ma allowed for orogen-parallel extension in the central Alps (Lepontine dome), associated with updoming of the isotherms. The Penninic realms of the central and western Alps differ significantly not only in deeper crustal architecture but also in the thickness of the seismogenic zone. Some of the earthquake foci (down to a depth of about 10–15 km are known to be associated with normal faulting within the axial zone of the Alps, while strike-slip and/or thrusting modes prevail in

the northern and southern forelands of the Alps. The cause of this normal faulting within the central parts of the Alps remains uncertain (gravitational collapse and/or buoyant rise of the lithospheric root). However, compression in both forelands suggests ongoing compressional coupling between the Adriatic and European Plates, although no focal solutions are available for the deep (>15 km) foci.

In summary, the three transects reveal major differences between the central Alps (Figure 21.1.3c) and western Alps (Figure 21.1.3a and b). As shown in Figure 21.1.1, the boundary between these two different segments of the Alpine chain coincides with the Rhone-Simplon line, which to this day continues to be seismically active and separates different modern stress domains.

21.1.5 Inferences Concerning Rheologic Behavior

The maximum depth of the seismogenic zone, which is assumed to coincide with the maximum depth of cataclasis (i.e., friction-controlled and dilatant deformation) is a widely disputed topic. Some partly speculative inferences can be made based on field observations and deductions from the geometry of the present-day deep structure of the Alps. Observations made by structural geologists focusing on the study of deformation microstructures indicate the onset of crystal-plasticity at different temperatures for different minerals under natural strain rates. Anhydrite (associated with the décollement horizon of Jura-type folding) may deform crystal-plastically above about 70°C; calcite exhibits significant non-cataclastic deformation above about 180°C; quartz starts to deform by crystal-plasticity above 270°C. Feldspar does not start to deform by crystal-plasticity below 450°C–500°C, but breakdown reactions in feldspar may promote reaction-enhanced ductility at lower temperatures, provided that water is available. Minerals such as hornblende and pyroxenes are more flow resistant than feldspar, and olivine does not start to deform crystal-plastically below 700°C.

At first, these data suggest a fairly shallow base for the seismogenic zone in the quartz-rich upper crust. However, elevated pore pressures are able to displace the brittle–plastic transition to greater depth (i.e., higher temperatures). On the other hand, deformation of more mafic lower crustal rocks is predicted to be controlled by cataclastic deformation at temperatures less than 450°C–500°C (i.e., down to Mohodepth for

an undisturbed geotherm within the foreland), assuming that the strength of these rocks is due to feldspar in the absence of significant amounts of quartz. Contrary to predictions based on the extrapolation of experimentally determined flow laws, therefore, lower crustal rocks may be flow resistant and deform by cataclastic processes. Hence, it is not surprising to find deep foci within lower crustal rocks, as shown in Figure 21.1.3 for the case of the Alpine forelands. However, lower crustal rocks may become weak within overthickened crustal roots of mountain belts, and/or if heat flow is elevated.

The geometry of the deep structure along the transects given in Figure 21.1.3 independently suggests that lower crustal rocks are flow resistant. This contrasts with a common assumption among geologists that the lower crust is generally “weak.” Lower crustal wedging demands the lower crust to remain little deformed (or undeformed) and calls for décollement horizons at the top, as well as at the base of the lower crust. Since quartz already starts to deform by crystal-plasticity above 270°C, the upper crust may easily detach from the lower crust. Given the high strength contrast between feldspar and olivine, detachment at the base of the lower crust may also occur, provided that temperatures of around 450°–500°C (onset of crystal-plasticity in feldspar) are reached within the lowermost continental crust.

It is interesting to note that the Adriatic lower crustal wedge in the NRP-20 East profile (Figure 21.1.3c) is presently aseismic, in contrast to the European lower crustal wedges in Figure 21.1.3a–b. This points to differences in the thermal regime between the central and western Alps. In case of the NRP-20 East profile the lower limit of seismicity roughly coincides with the 500°C isotherm, as predicted by thermal modeling along this transect. This independently supports the inference that the base of the seismogenic zone in the lower crust coincides with the cataclastic–plastic transition for feldspar near the 500°C isotherm.

21.1.6 Evolution of the Alpine System and Its Forelands in Time Slices

Our brief discussion of the history of the Alpine system in central and western Europe focuses on the evolution along the eastern (NFP-20 East) transect of Figure 21.1.3c, where the timing of events is best constrained. Figure 21.1.4 gives a timetable of orogenic activity, while Figure 21.1.5 depicts cross sections along this eastern transect for different time slices.

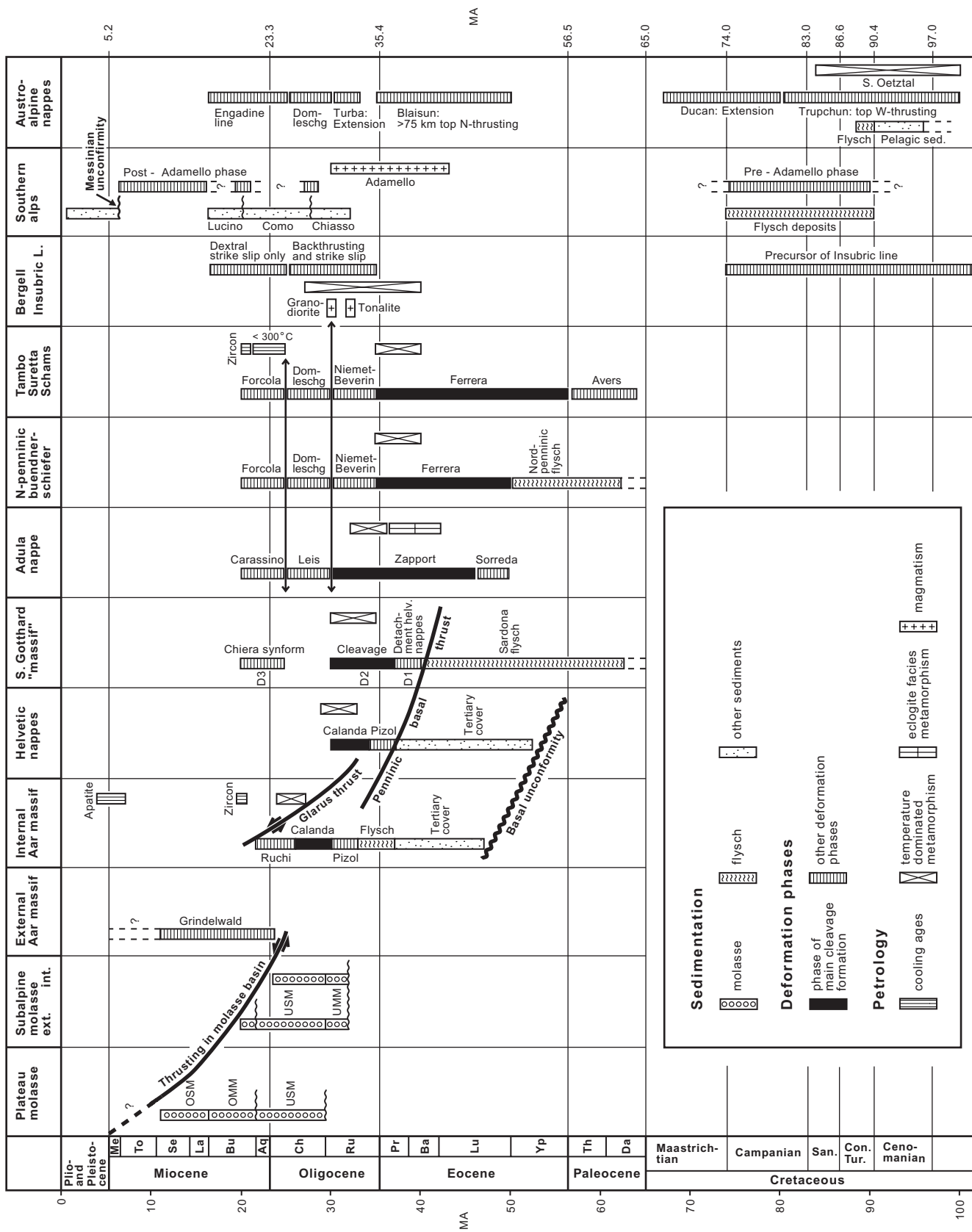


FIGURE 21.1.4 Correlation table showing an attempt to date deformation phases and metamorphism along the eastern transect.

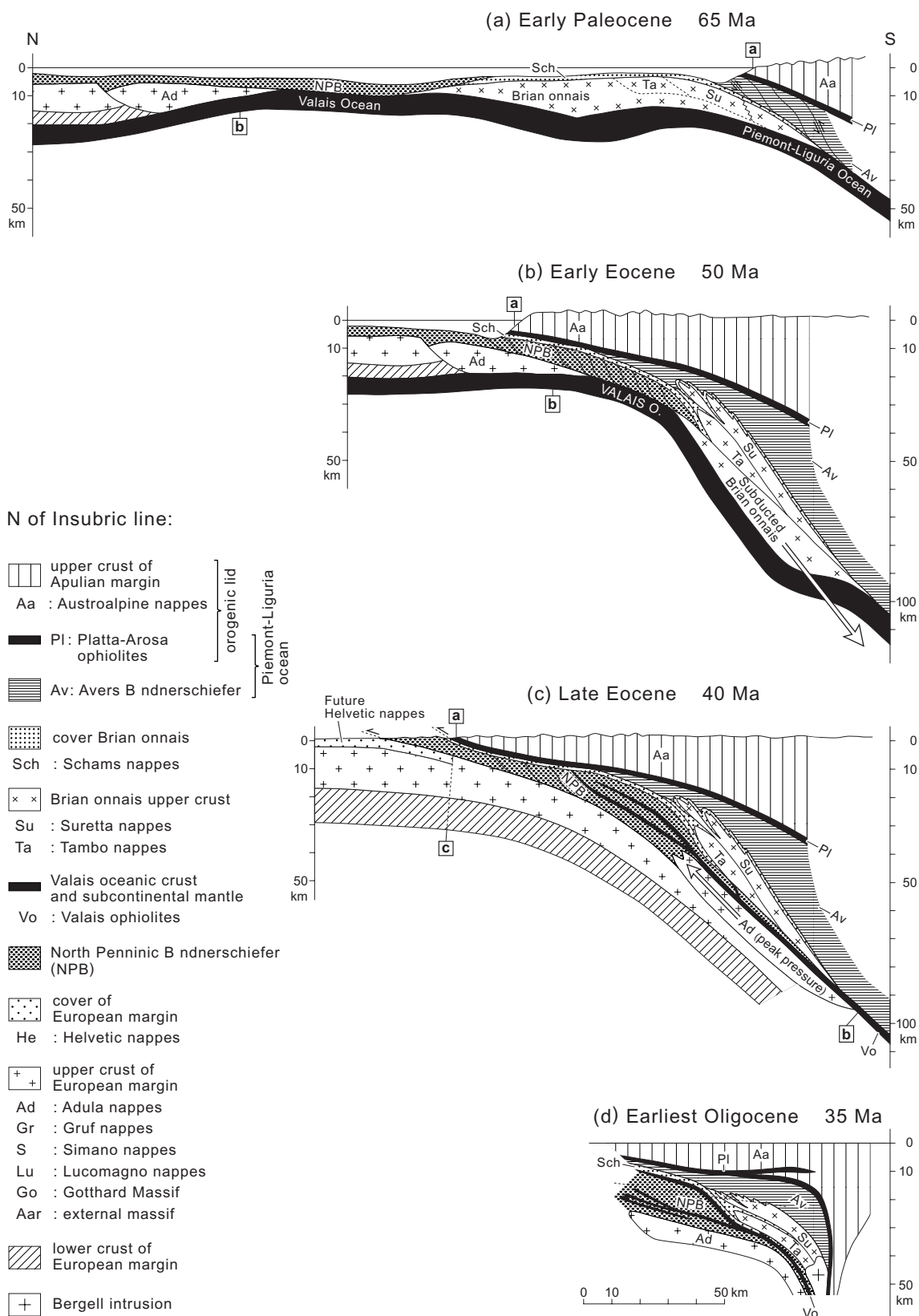


FIGURE 21.1.5 Scaled and area-balanced sketches of the kinematic evolution of the eastern central Alps from early Tertiary convergence [a and b], to collision [c], and postcollisional shortening [d–g].

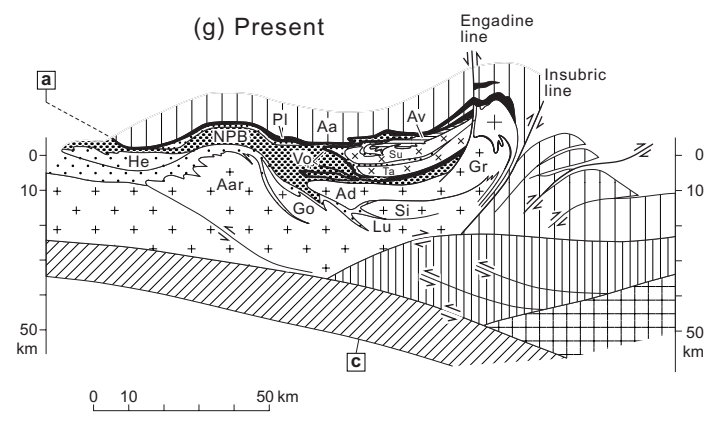
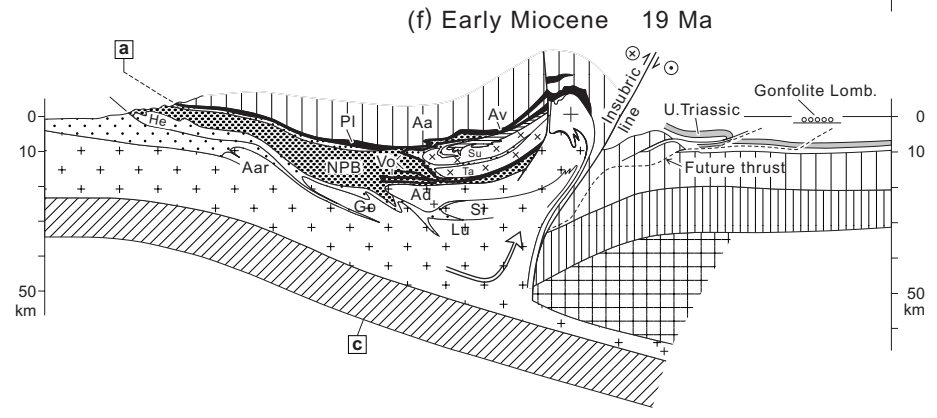
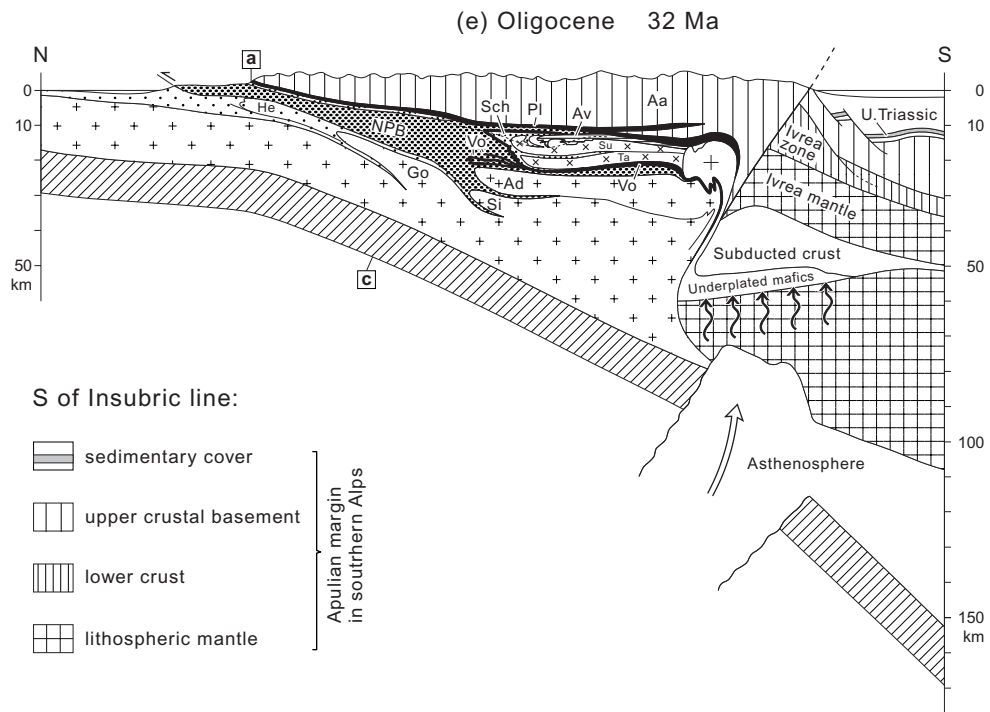


FIGURE 21.1.5 (Continued)

CRETACEOUS OROGENY Cretaceous (or Eo-Alpine) orogeny in the eastern Alps is regarded as independent and unrelated to Tertiary orogeny because of its different kinematic scenario (top to WNW, hence almost orogen-parallel thrusting) and because it is separated from Tertiary convergence by an extensional event during the Late Cretaceous (“Ducan extension” in Figure 21.1.4). Apart from the Austro-Alpine nappes, it only affects the Piemont-Liguria units of eastern Switzerland (Arosa-Platta), while the rest of the Penninic units remain largely unaffected by this orogeny, which did not propagate further to the west beyond eastern Switzerland, nor downsection into the Briançonnais units.

The attribution of a pre-Adamello phase in the southern Alps (the main deformation is of Miocene age) to Cretaceous orogenic activity is uncertain, but a precursor of the Insubric line must have been active because of the separation between the detached crustal flakes of the Austro-Alpine nappe system and the Adriatic lithosphere, which remained intact. However, the southern margin of the Piemont-Liguria margin represented an active margin, as documented by the accretionary wedge of the schistes lustrées and by the eclogitization of the Sesia unit at around the Cretaceous-Tertiary boundary.

During the various stages of Tertiary orogeny, the prestructured Austro-Alpine nappe system, together with the Arosa-Platta ophiolites, formed a rigid upper plate (referred to as “orogenic lid” in Figure 21.1.5a–d), of which the southern Alps formed part (not depicted in Figure 21.1.5a–c, but present at the southern margin of these figures).

EARLY TERTIARY CONVERGENCE AND SUBDUCTION (65–50 MA) During the Paleocene, the Briançonnais terrane enters the subduction zone, thereby closing the last remnants of the Piemont-Liguria Ocean in eastern Switzerland, the youngest sedimentary cover of which now forms an accretionary wedge consisting of the Avers Bündnerschiefer (Figure 21.1.5a). This southern ocean likely remained open for a longer period of time in the western Alps. After about 200 km of north-south convergence (13 mm/y) the distal margin of Europe (the future Adula nappe) enters the subduction zone at around 50 Ma, then closing the Valais Ocean (Figure 21.1.5b). Penetrative deformation during this time interval is largely restricted to the southernmost Penninic units, that is, the Briançonnais terrane (Tambo-, Suretta- and Schams nappes, see Figure 21.1.4) and the Avers Bündnerschiefer of the Piemont-Liguria Ocean (Figure 21.1.5b).

TERTIARY COLLISION (50–35 MA) During the middle and late Eocene (between Figure 21.1.5b and d), an

additional 200-km N–S plate convergence (corresponding to 15 mm/y) was taken up by the incorporation of the Valais Ocean and the distal European margin into a growing accretionary wedge below the orogenic lid formed by the Austro-Alpine nappes. Figure 21.1.4 illustrates the migration of deformation and metamorphic events towards the northern foreland, reaching the area of the future Helvetic nappes by the end of the Eocene. Note that a total of some 400 km of north-south convergence across the central Alps involves substantial sinistral strike-slip movement across the future western Alps. Hence, the western Alps formed under a sinistrally transpressive scenario during Early Tertiary convergence and collision, with west-directed movements postdating Tertiary collision (see postcollisional stage 1).

Since the Alpine nappes in Figure 21.1.5 exclusively consist of thin slices of upper crustal basement and/or its cover, detached from their lower crustal and mantle substratum, all European (and Valaisan) lower crust (including parts of the upper crust) must have been subducted together with the mantle lithosphere (Figure 21.1.5c). Hence, north-vergent nappe stacking during this collisional stage took place within an accretionary wedge that starts to grow as more non-subductable upper crustal granitic material of the European margin enters the subduction zone. Radiogenic heat production within this granitic basement, perhaps in combination with slab break-off (depicted in Figure 21.1.5e) leads to a change in the thermal regime and to Barrovian-type (i.e., Lepontine) metamorphism.

POSTCOLLISIONAL STAGE 1 (35–20 MA) Further growth of the accretionary wedge leads to retrothrusting of part of the material entering the subduction zone above the steeply north-dipping Insubric line (Figure 21.1.5e and f). A “singularity point” develops within the lower part of the upper crust, separating the subducting part of the European crust from that part of the wedge which is backthrust, sheared, and exhumed by erosion (this singularity point is near the bent arrow depicted in Figure 21.1.5f).

As can be seen from Figure 21.1.4, forward thrusting in the Helvetic nappes (i.e., the Glarus Thrust) is contemporaneous with retro- or backward thrusting along the Insubric line. The Alps evolve into a bivergent orogen, with a southern and northern foreland. Interestingly, the transition into bivergent thrusting coincides with increased rates of erosion due to the pop-up of the central Alps between fore- and retrothrusts, resulting in the transition from flysch-type to molasse-type sedimentation in the northern foreland.

North-south-directed plate convergence during this first postcollisional period amounts to about 60 km, slowing down to about 4.5 mm/y. In map view, this time interval coincides with the west-northwest-directed movement of the Adriatic Plate, now decoupled from the central Alps via dextral strike-slip movement along the Tonale line (about 100 km). Kinematically, the western Alps are now part of the west-northwest-moving Adriatic Plate and are separated from the central Alps along the Simplon ductile shear zone and later on by the Rhone-Simplon line (see Figure 21.1.1). Note that continental rifting in the Rhine and Bresse Grabens falls into this same time interval. However, this rifting is kinematically unrelated to shortening across the Alpine system, which remains in compression throughout.

POSTCOLLISIONAL STAGE 2 (20–7? MA) Continued crustal overthickening within the central part of the Alpine Orogen by bivergent (retro- and pro-wedge) thrusting eventually led to rapid propagation of the deformation front from the Insubric line towards the Po plain (southern Alps), as well as towards the northern foreland (thrusting at the base of the Aar Massif and within the southern Molasse Basin) at around 20 Ma. This is depicted in Figure 21.1.5e; the timing constraints are given in Figure 21.1.4. Regarding the southern Alps, deformation stopped at around 7 Ma (Messinian unconformity).

In the northern foreland, however, the situation is more complex. During the late Serravallian (12 Ma), deformation suddenly stepped further into the foreland, incorporating the western part of the Molasse Basin and the Jura Mountains into the orogenic wedge. While *décollement* along Triassic evaporites is recognized by most authors as being responsible for this forward stepping of the deformation front onto the northernmost Jura Mountains up to the southern Rhine and the Bresse Grabens, two questions remain unanswered:

- Did thin-skinned deformation stop at around 7 Ma in the Jura Mountains, that is, contemporaneous with foreland deformation in the southern Alps?
- How exactly did the arc of the Jura Mountains form? By clockwise rotation of the western part of the Molasse Basin and the northern Alps? Or by west to northwest directed indentation of the western part of the central Alps?

In regard to the first question we can argue that present-day deformation is thick-skinned, hence it is likely that Jura-folding was a short-lived event (12–7 Ma).

Regarding the second question we favor an indentation model, as there is evidence for counterclockwise rather than clockwise rotation of the Adriatic Plate during the Miocene. Assuming that relatively fast plate convergence across the Alpine system of Switzerland stopped at around 7 Ma, the 60-km plate convergence over the duration of this second postcollisional episode amounts to about 0.5 cm/y. Thus, plate convergence remained practically unchanged between 35 and 7 Ma. It is interesting to compare this figure of 5 mm/y to present-day shortening estimates across the Alpine system, as we do in the following section.

21.1.7 Recent Movements in the Upper Rhine Graben

Recent results from work in progress in the framework of EUCOR-UGENT program concerning the area of the Upper Rhine Graben in the Sundgau area west of Basel are shown in Figure 21.1.6. The Sundgauschotter have been deposited during a very short time interval from 3.2 to 2.6 Ma. Presently they outcrop within a 20-km wide corridor between the Vosges and the frontal Jura Mountains (see outlines of the base of the Sundgauschotter in Figure 21.1.6). The base of the Sundgauschotter forms an excellent reference horizon for inferring relative vertical movements during the last 3 m.y. or so (their basal part does not need to have been deposited everywhere 3.2 Ma, but they certainly must have been deposited before 2.6 Ma), provided that this basal contact is assumed to be near-horizontal at the time of deposition. The fact that these gravels were deposited in a braided river environment indicates that bases were nearly planar, with very minor slope from east to west.

The contour map of the bases of the Sundgauschotter (Figure 21.1.6) suggests substantial relative vertical uplift of the southernmost part of the depositional corridor with respect to the northernmost occurrences (in the order of 250 m). Moreover, two very pronounced *en-echelon* anticlines, gently folding the bases of the Sundgauschotter are inferred north of the Vendlincourt fold in the Rechésy area, these gentle folds being directly observable within Upper Jurassic limestones and Oligocene deposits below the bases of the Sundgauschotter. Note also that the bases of the Sundgauschotter are affected by at least part of the folding to be observed in the Ferrette fold.

The geometry of these folds, particularly in the area immediately east of Montbéliard, suggests thick-skinned reactivation of basement faults formed during Oligocene rifting. Hence, we propose a thick-skinned origin for the approximately north-northwest

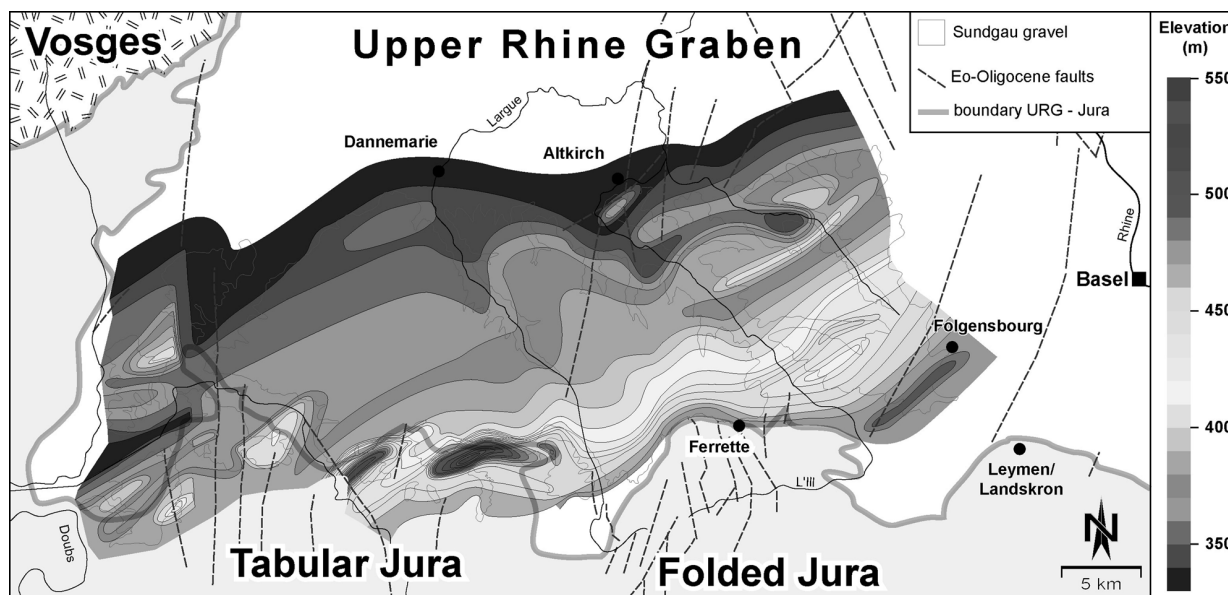


FIGURE 21.1.6 Contour map of the base of the Pliocene [3.2–2.6 Ma] Sundgau gravel deposits west of Basel. Assuming an originally planar base of these braided river deposits, the contours indicate folding with an amplitude of up to 200 m. This indicates substantial tectonic movements during the last 3 Ma, postdating thin-skinned Jura-type tectonics.

to south-southeast directed ongoing shortening, as indicated by the northernmost (post 3 Ma) folds in the Basel area affecting the Sundgauschotter, and suggest that this shortening is very probably going on at present. This pattern suggests that thin-skinned Jura folding may indeed have stopped around 7 Ma. Such a postulate is compatible with (1) the present-day stress field in the Jura Mountains, as determined by in situ stress measurements, indicating that the Jura belt is no longer an active thin-skinned fold-and-thrust belt, (2) the historical Basel earthquake, which reactivated a deep-seated basement fault, and (3) the occurrence of intracrustal earthquakes within the Molasse Basin (Figure 21.1.3c).

21.1.8 Closing Remarks

To some extent, the considerable complexities in structure and evolution of the European Alps, outlined in this essay, reflect the fact that our knowledge of their surface geology and deep structure is exceptionally detailed when compared with that of other orogens. Also, the Alps are particularly well exposed. Furthermore, the existence of along-strike culminations, such as the Lepontine dome (Figure 21.1.1), allows for along-strike projections of deep-seated structures to laterally adjacent areas. Such lateral (or axial) projections may cover a depth interval of up to 30 or 40 km (e.g., Figure 21.1.3c). Such projections have been a classical

tool of Alpine geology since the pioneering work of Argand in the beginning of the twentieth century.

Our knowledge concerning the deep structure is relatively recent and results from a series of geophysical transects carried out cooperatively by an international group of French, Italian, Swiss, German, and Austrian scientists (ECORS-CROP, NFP-20, and very recently TRANSALP in the eastern Alps). The combination of geologic and geophysical data offers the unique opportunity to unravel the crustal structure of this orogen from its former (now eroded) surface 10 km above sea level, down to the crustal roots at more than 50 km depth.

However, in spite of the “model” character the Alps have always had, there are also good reasons to believe that they are special and that many of their features should not be extrapolated to other parts of the world. Features such as, for example, the very considerable along-strike variations in the overall architecture of the orogen, the superposition of two orogenies (Cretaceous and Tertiary) in one mountain belt, and, the former existence of three oceanic domains (Valais, Piemont-Liguria, and Neotethys Oceans) may be rather special.

We will not know for certain how special the Alps are before we have data in comparable detail from other orogens. In the meantime, the Alps will continue to serve as a case study concerning the integration and interpretation of a very large set of geologic and geophysical data.

ADDITIONAL READING

- Beaumont, C., Fullsack, P. H., and Hamilton, J., 1994. Styles of crustal deformation in compressional orogens caused by subduction of the underlying lithosphere. *Tectonophysics*, 232, 119–132.
- Becker, A., 1999. In situ stress data from the Jura mountains—new results and interpretation. *Terra Nova*, 11, 9–15.
- Burkhard, M., 1990. Ductile deformation mechanisms in micritic limestones naturally deformed at low temperatures (150–350°C). In Knipe, R. J., et al., eds., *Deformation Mechanisms, Rheology, and Tectonics, Geological Society Special Publication*, 54, 241–257.
- Burkhard, M., and Sommaruga, A., 1998. Evolution of the western Swiss Molasse basin: Structural relations with the Alps and the Jura belt. In Mascle, A., et al., eds., *Cenozoic Foreland Basins of Western Europe, Geological Society Special Publication*, 134, 279–298.
- Froitzheim, N., Schmid, S. M., and Frey, M., 1996. Mesozoic paleogeography and the timing of eclogite-facies metamorphism in the Alps: A working hypothesis. *Eclogae Geologicae Helveticae*, 89, 81–110.
- Giamboni, M., Ustaszewski, K., Schmid, S. M., Schumacher, M., and Wetzel, A. (submitted). Plio-Pleistocene transpressional reactivation of Paleozoic and Paleogene structures in the Rhine-Bresse transform zone (Northern Switzerland and Eastern France). *International Journal of Earth Sciences*.
- Meyer, B., Lacassin, R., Brulhet, J., and Mouroux, B., 1994. The Basel 1356 earthquake: which fault produced it? *Terra Nova*, 6, 54–63.
- Schmid, S. M., Pfiffner, O. A., Froitzheim, N., Schönborn, G., and Kissling, E., 1996. Geophysical-geological transect and tectonic evolution of the Swiss-Italian Alps. *Tectonics*, 15, 1036–1064.
- Schmid, S. M., Pfiffner, O. A., and Schreurs, G., 1997. Rifting and collision in the Penninic zone of eastern Switzerland. In Pfiffner, O. A., et al., eds., *Deep Structure of the Alps, Results from NFP 20*, Birkhauser Verlag.
- Schmid, S. M., and Kissling, E., 2000. The arc of the western Alps in the light of geophysical data on deep crustal structure. *Tectonics*, 19, 62–85.

21.2 THE TIBETAN PLATEAU AND SURROUNDING REGIONS—An essay by Leigh H. Royden and B. Clark Burchfiel¹

21.2.1 Introduction	525	21.2.5 Extension of the Tibetan Plateau	532
21.2.2 Precollisional History	525	21.2.6 Closing Remarks	533
21.2.3 Postcollisional Convergent Deformation	527	Additional Reading	533
21.2.4 Crustal Shortening and Strike-Slip Faulting	530		

21.2.1 Introduction

The collision of India with Asia about 50 Ma and their subsequent convergence (Figure 21.2.1) has produced a spectacular example of active continent-continent collision. This immense region of continental deformation, which includes the Tibetan Plateau and flanking mountain ranges, contains the highest mountain peaks in the world, with many peaks rising about 8000 m (the **Himalaya**). Indeed so many mountain peaks rise above 7000 m that many of these remain unnamed and uncounted. The **Tibetan Plateau** proper stands between about 4000 and 5000 m in elevation and covers a region about 1000 by 2000 km², and most of it has remarkably little internal relief. It is sobering to compare the size of this region to other mountain ranges; for example, the crustal mass of the Tibetan Plateau above sea level is about 100 times greater than that of the western Alps.

The first synthesis of the tectonic evolution of southeast Asia, including the Himalaya and the Tibetan Plateau, was constructed by the Swiss geologist Emile Argand in 1924. Many of our current ideas about this region are contained in his book “La tectonique de l’Asie,” which remains today one of the truly creative and imaginative works in the earth sciences. Unfortunately, from about World War I until about 1980, much of this region (in China and the former Soviet Union) was closed to foreign scientists and only since the 1980s has the area been open to international research. Thus much of our knowledge of the geology of the Tibetan plateau and surrounding regions must be considered as largely reconnaissance, particularly when compared to regions like the relatively small western

Alps, where geologic research has been conducted by generations of earth scientists for more than 150 years.

In spite of our relatively sketchy knowledge of the Tibetan region, this exotic, remote, and inaccessible area has long excited the interest of scientists and non-scientists alike. For earth scientists, the rise of the Tibetan Plateau and the creation of the flanking mountain ranges and basins is a dramatic example of continental convergence and collision (Figure 21.2.1). It is exciting because of the youthful nature of the structures that accommodate deformation and the exceedingly rapid rates at which deformation is occurring. One of the great attractions of geologic study in this region is the great promise that it holds for enhancing our knowledge of continental deformation processes, as exemplified by an enormous list of still-unanswered questions (including crust–mantle interactions, driving mechanisms for local and regional deformation, and the interdependence of mountain building and global climate). In this essay we will try to summarize briefly what is known about the deformation history of the Tibetan Plateau and surrounding regions, outline some of the hypotheses and controversies that are unresolved today, and discuss some of the fundamental questions that will direct the future of geologic and geophysical studies in this region.

21.2.2 Precollisional History

At the beginning of Mesozoic time, all of the continental land masses were assembled into a giant continent called Pangea. At this time a Mesozoic ocean, called Tethys, formed a huge embayment into Pangea from the east and separated the part of Pangea that is now Eurasia (called Laurasia) from the part of Pangea that is now the continents of Africa, India, Australia,

¹Massachusetts Institute of Technology, Cambridge, MA.

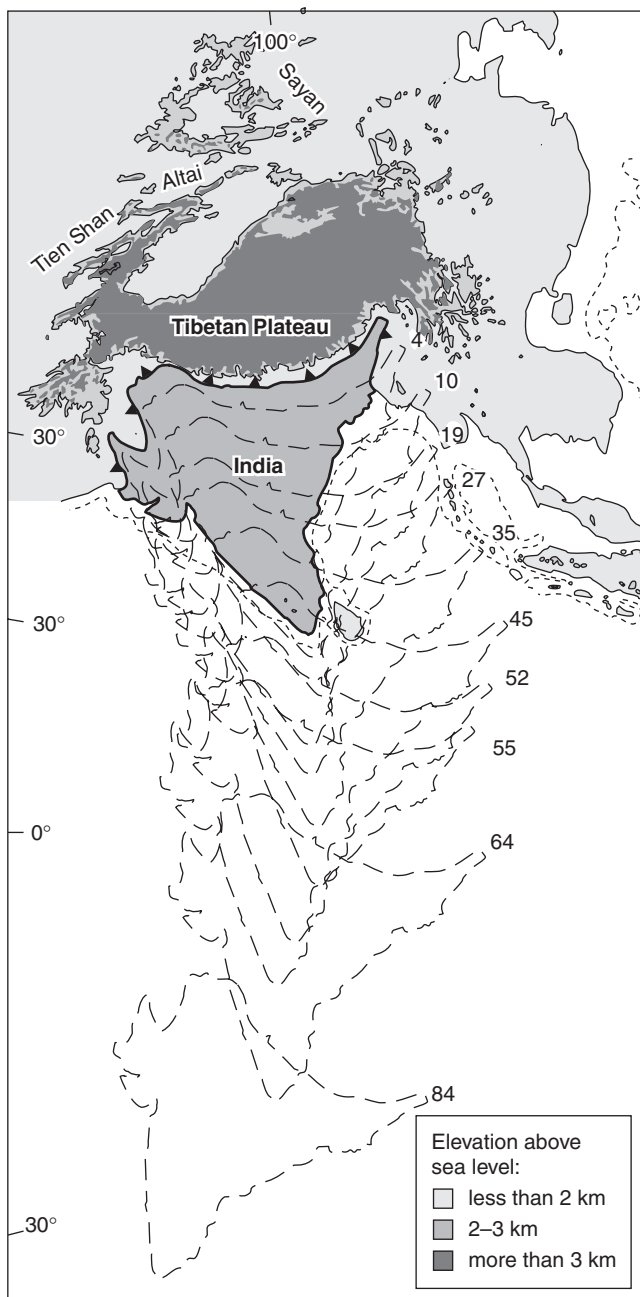


FIGURE 21.2.1 Generalized topographic map of Southeast Asia showing elevation above sealevel [from Burchfiel and Royden, 1991] and positions of India with respect to Asia from Late Cretaceous time until the present. Numbers refer to millions of years before the present. Note the decrease in convergence rate from about 100 mm/y to about 50 mm/y at about 50 Ma.

and Antarctica (called Gondwana). Tethys was perhaps a few hundred kilometers wide in the westernmost Mediterranean region, but widened toward the east, so that, at the longitude of Tibet, Tethys was approximately 6000 km wide.

At the longitude of Tibet, several sizable continental fragments collided with Asia and became accreted



FIGURE 21.2.2 Major fragments in Southeast Asia during Late Paleozoic, Mesozoic, and Early Cenozoic time. The sutures between fragments are shown by barbed lines with the barbs indicating the upper plate of the subduction system. The suture between the Qangtang and Songpan Ganze [SG] fragments is of Mesozoic age and is thought to represent the closure of the Paleotethys Ocean. All sutures north of this are Paleozoic. The suture south of the Lhasa block is the Indus-Tsangpo suture, and represents the closure of Neotethys. A, island arc fragments, V, location of Cretaceous-Early Tertiary arc volcanism. Location of cross section in Figure 21.2.3 is also shown.

to the Asian continental margin before the main collision between India and Asia (Figure 21.2.2). These continental fragments were rifted from Gondwana and moved northward. As each continental fragment was rifted from Gondwana, it opened a new ocean region between itself and Gondwana. At the same time, the old ocean north of each fragment was closed by subduction. For example, the first fragment to collide with Asia closed the early Mesozoic Tethys (more properly called Paleotethys). The Indian subcontinent is the last fragment to have rifted off of Gondwana and as it moved northward, it opened the Indian Ocean to the south of India and closed the Neotethyan ocean to the north. It is the closure of this Neotethyan ocean and the collision of India with Asia that has produced the 2500-km long Alpine-Himalayan mountain chain, along which continental collision and convergence are occurring today, and many parts of it are still incom-

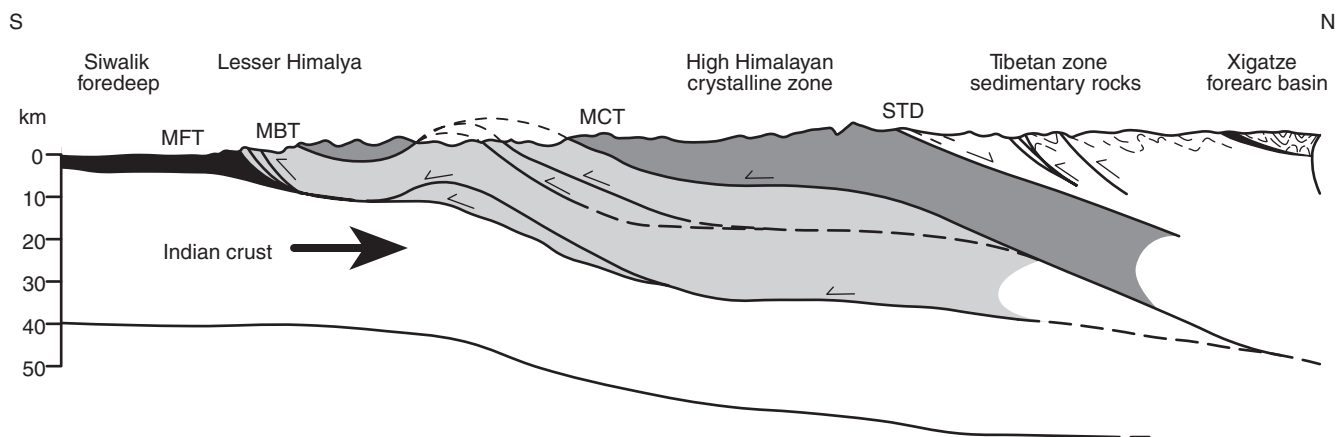


FIGURE 21.2.3 Schematic cross section through the central Himalaya (location in Figure 21.2.2). The Miocene-Quaternary molasse [heavy dots] of the modern foredeep basin are contained within the outer thrust sheets near the Main Frontal Thrust (MFT). Light shading represents low-grade metamorphic rocks north of the Main Boundary Thrust (MBT) and south of the Main Central Thrust (MCT). Dark shading represents high-grade metamorphic and crystalline rocks north of the MCT. These are separated from sedimentary rocks of the Tibetan zone (in white) by the normal South Tibetan Detachment (STD). Also shown are the Cretaceous Xigatze forearc deposits that rest on an ophiolitic basement (black sliver).

pletely closed (e.g., the Mediterranean region still contains Mesozoic seafloor of Tethys).

Prior to the main collision of India with Asia in early Tertiary time, several thousand kilometers of the Neotethys ocean floor was subducted beneath Asia along a north-dipping subduction boundary. Subduction was extremely rapid, resulting in convergence between India and Asia at about 100 mm/y. Evidence for precollisional convergence and deformation is recorded within the Himalayan mountain belt and in the southernmost part of the Tibetan Plateau. For example, within the central part of southern Tibet, Jurassic ophiolites obducted onto the Asian continental margin attest to the existence of an ancient ocean region between India and Asia. A late Cretaceous forearc sequence records subduction continuing at least into the Cretaceous (Figure 21.2.3). North-dipping subduction of an oceanic region is also recorded by a late Cretaceous to early Cenozoic volcanic arc along the southern margin of Asia (e.g., the Gandese batholith near Lhasa in south-central Tibet, which lies just north of the Xigatze forearc basin in Figure 21.2.3). Volcanism in this arc shut off in Eocene time, presumably reflecting the time of collision and the cessation of subduction of oceanic lithosphere. In the western Himalaya, precollisional subduction of Tethys must have occurred partly offshore, south of the Asian continental margin, because a Jurassic-Cretaceous volcanic arc (the Kohistan arc) was developed in a marine environment, and subsequently collided with the

southern margin of Asia in latest Cretaceous time, somewhat before the time of the main India-Eurasia collision. It is likely that events before and around the time of collision were very complicated, but at present the geologic data needed to unravel these events has not been obtained so the early evolution of the Himalayan system looks deceptively simple.

21.2.3 Postcollisional Convergent Deformation

At about 50 Ma India collided with Asia, and at about the same time the convergence rate between India and Asia slowed from about 100 mm/y to about 50 mm/y. Since that time India has continued to move northward relative to stable Eurasia at about 50 mm/y, giving a relative convergence of about 2500 km since the time of collision, and shortening and thickening the crust of Asia to produce the elevated Tibetan Plateau. Today, the continental crust beneath the high-standing plateau and flanking mountains is about 70 km, nearly double the more normal values of 30–40 km for continental crust. It is remarkable that in 1924, long before the advent of plate tectonics, Emile Argand already understood that an ocean had closed between India and Asia and that subsequent convergence between India and Eurasia has caused the intracontinental deformation of Southeast Asia. However, it is only in the last few decades that knowledge of the magnetic anomalies on the seafloor and paleomagnetism have allowed

scientists to reconstruct the motions of India with respect to Asia in a quantitative manner, and to calculate the width of the subducted ocean.

The boundary where India and Asia first collided, often referred to as the Indus-Tsangpo suture, is marked by a discontinuous belt of ophiolites, *mélange*, and forearc sedimentary rocks of the Gandese magmatic arc. It has been impossible to reconstruct the early collisional history of this zone because postcollisional deformation involving north-directed backthrusting, strike-slip faulting, and normal faulting has completely obscured the older collisional structures. There is also very little information about postcollisional deformation within the Himalayan belt prior to about 250 Ma, although in the western Himalayan chain geologists have identified early Cenozoic metamorphism events dated at around 35–45 Ma. This indicates that thrust faulting and crustal shortening were active in the western Himalaya at about this time, and suggests that the creation of high topography within the western Himalaya may have already been underway. However, as we shall see, the time at which high topography developed within most of the Himalaya and Tibet is extremely controversial, not least because of its implications for global climate change.

The evolution of the Himalayan Orogen is better known from about 25 Ma to the present, although there is still much that we do not know about the orogen. A schematic north-south cross section through the Himalaya and into southern Tibet (Figure 21.2.3) shows that regional shortening is thought to have been taken up on thrust faults within sedimentary rocks north of the crest of the Himalaya (called the Tibetan zone sedimentary rocks) and on three major north-dipping thrust faults south of the crest of the Himalaya, the Main Central Thrust (MCT), the Main Boundary Thrust (MBT), and the Main Frontal Thrust (MFT). All of these structures appear to be roughly continuous for more than 200 km along the entire length of the Himalayan chain. Shortening across the Himalaya was further accommodated by intense ductile strain within high-grade and crystalline rocks, as well as by folding and thrusting along less important faults.

The oldest of these thrust faults are probably within the Tibetan sedimentary sequence, but their age remains uncertain. The MCT, which may be younger, carries the high-grade crystalline and metamorphic rocks of the High Himalayan zone over the lower grade to unmetamorphosed sedimentary rocks of the Lesser Himalaya. So far, only one date has been obtained for thrusting on the MCT. This date was obtained on rocks just south of Qomolangma (Mt. Everest) in central Tibet, indicating that the MCT

was active at 21 Ma. However, we do not yet know how long before or after this time the MCT was active, although in most places it is not active today. In addition, we do not know if this data can be extrapolated to the east or west along the strike of the MCT; it is possible that although the MCT appears continuous along the length of the Himalaya, it is of different ages and different character along different parts of the belt. Metamorphic pressure and temperature data from central Tibet show that at 20–25 Ma the MCT was at a depth of about 30 km and that temperatures of High Himalayan rocks near and just above the MCT were at least 500°C–650°C. Thus the rocks of the High Himalaya must have been brought to the surface from a depth of 30 km during the last 30 m.y.

South of the MCT, the MBT carries the low-grade to unmetamorphosed rocks of the Lesser Himalaya southward over mainly Cenozoic sedimentary rocks. In some places there is evidence that the MBT may be currently active, but the main shortening and convergence across the Himalaya today is probably absorbed by motion along the structurally lower MFT and by folding within its hanging wall. The MFT marks the southern limit of deformation along most of the Himalayan chain and carries rocks and sediments of the Himalaya southward over the Ganga foredeep basin. Sediments being deposited in the Ganga Basin today are similar to those now exposed by erosion within the Himalayan foothills, suggesting that the latter were also deposited in a foredeep position in front of the frontal thrust faults, and have been subsequently incorporated into the thrust belt.

Seismic studies and examination of the rate of advance of the Ganga Basin southward over the Indian foreland indicate that about 10–25 mm/y of shortening is currently being taken up by thrust faulting and shortening within the Himalaya. Seismic studies also show that the main active thrust fault beneath the Himalaya dips gently northward by about 10°, until it becomes aseismic at a depth of about 18 km. At these depths we assume that this active, gently dipping thrust boundary is somewhat analogous to the Early Miocene MCT, but of course there are no direct observations to support this hypothesis.

Because the current rate of convergence between India and stable Eurasia averages about 50 mm/y, this means that only about one-quarter to one-half of the convergence between India and Eurasia is accommodated by shortening within the Himalaya. The rest must be taken up to the north within and around the margins of the Tibetan Plateau. The way in which the remaining convergence is absorbed remains a highly controversial topic, for which there are perhaps more

models than data. However, considerable amounts of convergence are clearly absorbed by thrusting and shortening within mountain belts that lie north of the plateau, particularly in the Pamir, Tien Shan, Quilian Shan, and southern Ningxia (e.g., Madong Shan) thrust systems (Figure 21.2.4). The rates of shortening across these belts are not very well known, but they are probably at least 10 mm/y, perhaps considerably more. Although shortening across the Pamirs began in Early Cenozoic time, shortening across the other northern thrust belts probably began only in Late Miocene to Quaternary time. The onset of thrusting in these regions is primarily constrained by stratigraphic data because Cenozoic metamorphic rocks are not found in any of these young thrust belts.

The onset of uplift and shortening along the northern and northeastern margins of Tibet is probably best regarded as the northward growth of the Tibetan Plateau. We can only surmise that the early history of rocks now contained within the central part of the plateau might have been similar to those now being incorporated into the plateau by shortening along its northern boundary. It is clear that the northward growth of the plateau has not been a smooth process. The map of present-day deformation north of the plateau shows a very irregular pattern of thrust belts, with a huge undeformed region, the Tarim Basin, sandwiched between the Tibetan Plateau proper and the very active region of shortening within the Tien Shan, and overthrust from all sides. Active shortening, albeit at much lesser rates, also occurs far to the north within the Altai Ranges in north China and Mongolia. The northward growth of the plateau has not been a smooth process in time either. For example, shortening appears to have begun sometime in late Pliocene to early Quaternary time in much of the northeastern portion of the plateau. However, examination of individual ranges and thrust belts in this region does not reveal a steady northward progression of the deformation front, but rather a more haphazard onset of shortening, in part caused by the reactivation of pre-Cenozoic structures. On a scale of hundreds of kilometers, the deformation along the northern margin of Tibet appears to be controlled largely by strength heterogeneities and preexisting structural trends within the Asian lithosphere.

The structure of the thick crust beneath the Tibetan Plateau is not known, although a number of different hypotheses have been presented, each linked to a different model for plateau growth. On one hand, a number of authors, beginning with Argand, believe that the crust beneath the Tibetan Plateau has been doubled by underthrusting of the Indian crust and lithosphere beneath the Asian crust (Figure 21.2.5). In some of

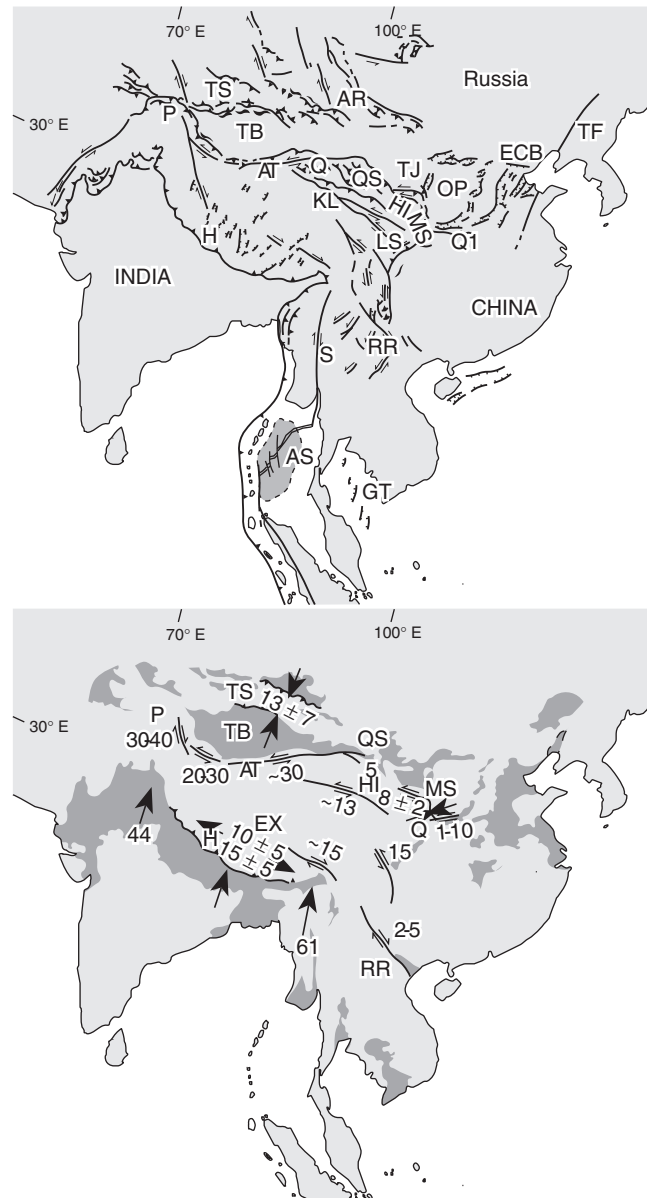


FIGURE 21.2.4 (a) Generalized Cenozoic tectonic map of Southeast Asia. Horizontal arrows indicate sense of slope on strike-slip faults; barbed lines indicate thrust faults in the continental areas and subduction zones in the oceanic areas, with barbs on the upper plates; and ticked lines indicate normal faults. Lunate shapes are folds. AR = Altai Range, AS = Andaman Sea, AT = Altyn Tagh Fault, ECB = East China Basins, GT = Gulf of Thailand, H = Himalaya, HI = Haiyuan Fault, KL = Kun Lun Fault, LS = Longmen Shan, MS = Madong Shan, OP = Ordos Plateau, P = Pamirs, Q = Qaidam Basin, QS = Qilian Shan, Q1 = Qinling Mountains, RR = Red River Fault, S = Sagaing fault zone, TB = Tarim Basin, TF = Lan Lu fault zone; TJ = Tianjin Shan, TS = Tien Shan, X = Xianshuhe Fault, Y = western Yunnan. (b) Slip rates [in mm/y] on active faults within Southeast Asia. Reversed arrows identify slip direction on strike-slip faults. Medium black arrows that diverge indicate areas and directions of extension; medium black arrows that converge indicate areas of shortening across thrust faults (and folds) with barbed lines. Large north-pointing arrows south of the Himalaya indicate direction and magnitude of present convergence between India and northern Asia.

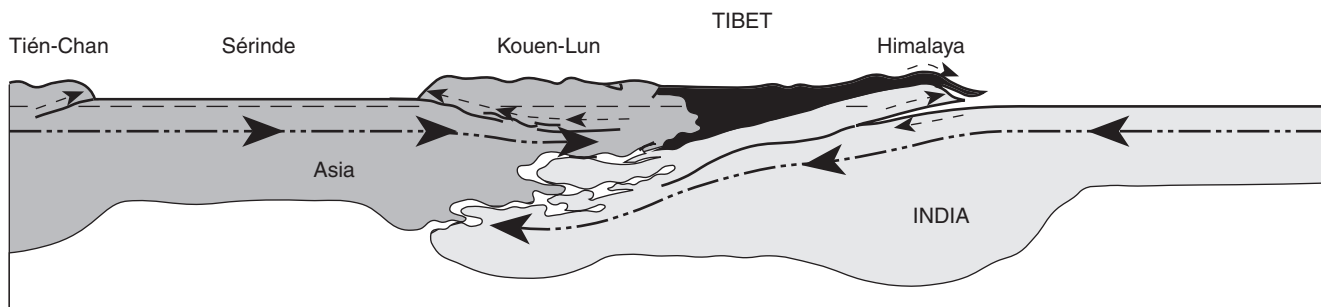


FIGURE 21.2.5 North-south cross section through Tibet and the Himalaya published by Emile Argand in 1924. Modern interpretations have not added much to our understanding of the deeper structure beneath Tibet. Light gray is Indian crust, dark gray is Asian crust, mantle material is white.

these models it is suggested that essentially no deformation of the upper (Asian) crust has occurred, while others include moderate amounts of upper crustal deformation or deformation only within the northern part of the plateau. In contrast to the first model is the suggestion that the Indian lithosphere only extends beneath the Himalaya and southernmost Tibet, and that the doubling in thickness of the Tibetan crust was mainly the result of shortening and thickening of the Tibetan crust due to the India-Eurasia collision. To date there are little conclusive data that bear directly on this problem.

21.2.4 Crustal Shortening and Strike-Slip Faulting

A heated controversy surrounds two extreme, and basically incompatible, views of how the India-Eurasia collision and crustal shortening in Tibet are related to Cenozoic deformation throughout much of Southeast Asia. One group of workers, in a ground-breaking set of papers, suggested that the postcollisional convergence of India and Asia has been responsible for most of the Cenozoic deformation of Southeast Asia. They argued that although the Tibetan Plateau did indeed form by crustal shortening, the total crustal mass beneath the plateau is too little (by about 30%) to account for all of the convergence between India and Eurasia since the time of the collision. Using earthquake seismology and newly available satellite imagery, they suggested that the remaining convergence was accommodated by eastward ejection of continental crust away from the plateau and out of the way of India as it moved northward toward Siberia (Figure 21.2.6a). Later, experiments on plasticine were used to suggest that eastward extrusion of continental fragments was also responsible for the Early Cenozoic extension within the South China Sea and the Gulf of

Thailand. This requires displacements of hundreds to a thousand kilometers on the large strike-slip faults within the Tibetan Plateau.

In a very different model, a numerical computer simulation was used by other workers to model Asia as a viscous sheet deformed by a rigid indenter (India). These numerical models predict a zone of shortening and thickening crust that grows northward and slightly to the side of the northward-moving indenter (Figure 21.2.6b). Because no deformation occurs beyond the boundaries of this zone of crustal shortening and thickening in front of the indenter, they have argued that only the Tibetan Plateau and flanking mountain belts have resulted from the collision of India and Asia. In this interpretation, the other regions of Cenozoic deformation in Southeast Asia are mainly unrelated to the India-Eurasia collision.

Both of these interpretations are based mainly on models, although the early work incorporated the geologic and geophysical data available at that time. What do current data say about this debate? The study of slip-rates on active faults shows that continental blocks within Tibet are indeed moving eastward at rates between 10 and 30 mm/y, as predicted by one set of models. However, these motions record only a snapshot of present day motions and do not answer the question of how much eastward ejection of material has occurred within Tibet. So far, geologic mapping has determined the total offset on the large strike-slip faults in only a few places. These data show about 15 km of left slip on the Haiyuan Fault, 200 km of left slip on the Altyn Tagh Fault, and 50 km of left slip on the Xianshuhe Fault (see Figure 21.2.4 for locations). Thus, while all of these strike-slip faults are moving very fast, they are also very young, and the total offset on these faults, while large, is not of the magnitude predicted by some models. While a definitive test of the extrusion model is not yet possible, the data sug-

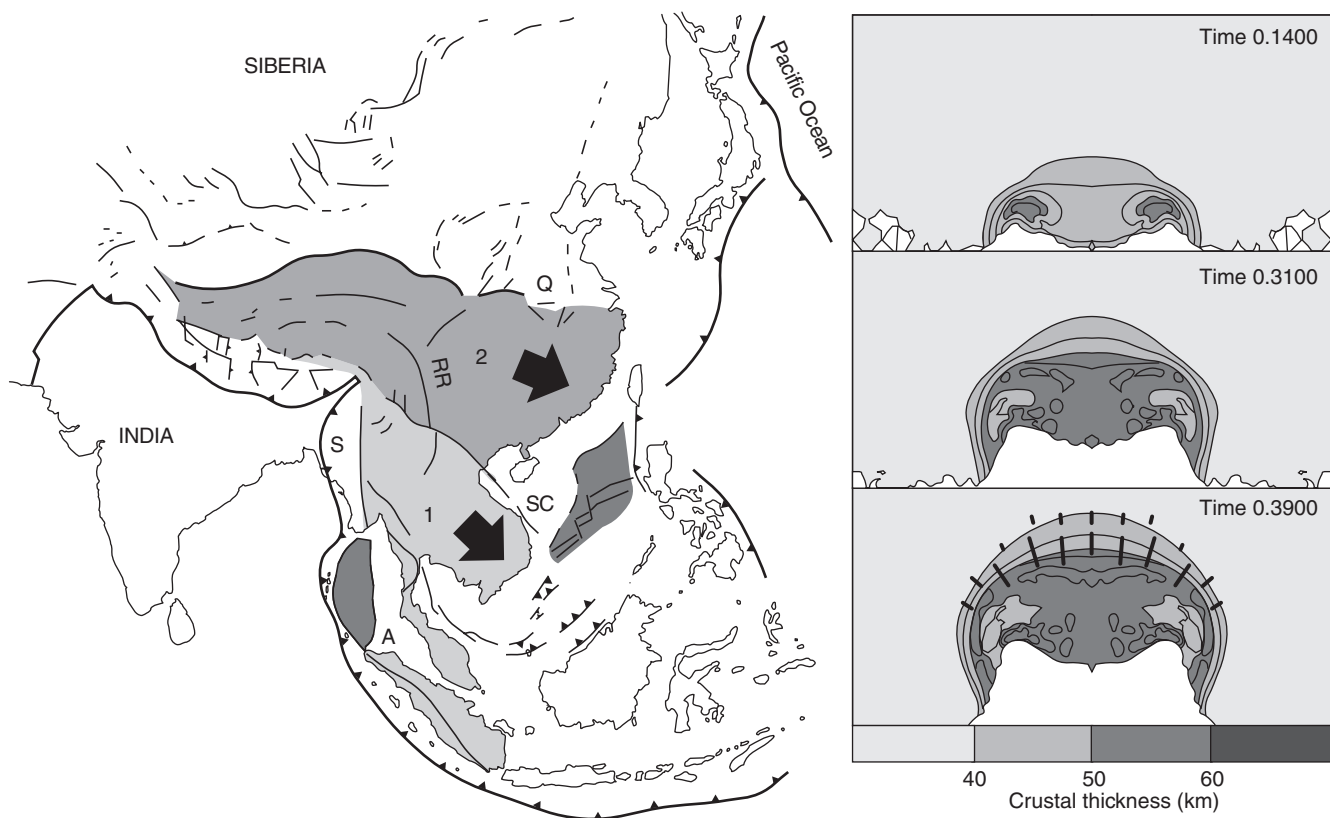


FIGURE 21.2.6 Two interpretations of the tectonic framework of Southeast Asia.

(a) The interpretation of Tapponnier and coworkers, which emphasizes the eastward extrusion of two large crustal fragments bounded by major strike-slip faults as a result of the India-Eurasia convergence. In this interpretation, eastward movement of these fragments results in the extension on the Southeast Asian continental shelf and creation of oceanic crust in the South China Sea. The first crustal fragment to move [1] is indicated by a large arrow and shown in light gray and the second to move [2] is indicated by another large arrow. RR = Red River Fault, S = Sagaing Fault, SC = South China Sea, A = Andaman Sea. (b) The interpretation of England and Houseman shows the progressive development of topography in Asia by computer modeling of a rigid indenter (India) deforming a viscous sheet (Asia). This model suggests that India-Eurasia may have little if any effect east or west of the Tibetan Plateau, and so is very different from that of Tapponnier. Contours are of increasing crustal thickness at different times [times are dimensionless, but the bottom panel would approximately correspond to the present topography of Tibet].

gest that while extrusion does occur, it is of much smaller magnitude than that predicted by this model.

Strike-slip faults within the Tibetan Plateau also have a very interesting relationship to thrust faulting and crustal shortening occurring around the margins of the plateau. At the eastern end of some of the strike-slip faults, they merge with, or end against, the active thrust faults that rim the margins of the plateau. This is best illustrated for the Haiyuan strike-slip fault in the northeastern corner of the plateau, where geologic mapping shows that 15 km of left slip on this east-west trending thrust fault is absorbed by 15 km of shortening on a north-south trending thrust belt in the Liupan Shan (Figures 21.2.4 and 21.2.7). In addition, the onset of strike-slip faulting on the Haiyuan Fault is of

approximately the same age as the onset of shortening in the Madong Shan (early Quaternary). Thus the left-slip motion on the strike-slip faults is absorbed by thrusting at the plateau margins, suggesting that lateral extrusion of crust within the plateau does not extend beyond the topographically high region.

Probably one of the reasons that so much emphasis has been placed on strike-slip faulting within the Tibetan plateau and surrounding regions is that many of the studies of active faulting have used satellite photos to identify important faults. Faults that dip steeply and are straight show up very well on these photos, while gently dipping faults with a complicated outcrop pattern can be difficult to recognize. Therefore the strike-slip faults within the plateau were recognized

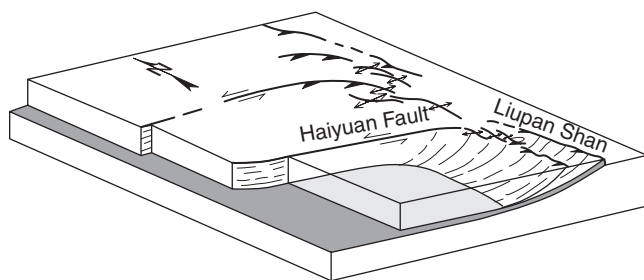


FIGURE 21.2.7 Schematic block diagram illustrating that strike-slip faults [such as the Haiyuan Fault shown here] end against thrust belts that bound the margins of the Tibetan Plateau [such as the Liupan Shan], and indicating how both thrust faults and strike-slip faults may be detached from the deeper crust by a zone of detachment within the mid-crust. See Figure 21.2.4 for locations.

very quickly, while many of the important thrust faults have probably not yet been identified. Another problem is that large amounts of shortening around the margins of the plateau occur not only by faulting, but by folding, which is aseismic and not recorded by earthquakes. Thus it is easy to underestimate the rates of crustal shortening relative to the rates of strike-slip faulting from looking at first-motions from earthquakes on and around the plateau.

21.2.5 Extension of the Tibetan Plateau

Not all of the deformation of the Tibetan Plateau is compressional. A series of north-south striking grabens in southern Tibet is accommodating active east-west extension of the plateau at about 10 mm/y (Figure 21.2.4). These grabens are very young, with extension beginning at about 2 Ma, giving a total amount of east-west extension of about 20 km. The significance of this extension is unclear and is also somewhat controversial. Some workers relate the east-west extension to the eastward extrusion of material from the Tibetan Plateau and argue that the presence of east-west extension supports their interpretation. In contrast, others have suggested that east-west extension of the plateau records the delamination (falling off) of the mantle lithosphere beneath the plateau sometime in the Late Miocene or Pliocene. They argue that the removal of the dense lithosphere from beneath the plateau caused uplift of the plateau surface (as cold, dense mantle lithosphere was replaced by hot, buoyant asthenosphere), and that the surface elevation of the plateau is now decreasing by east-west extension within the plateau. At present, the significance of these north-south trending grabens remains highly uncertain

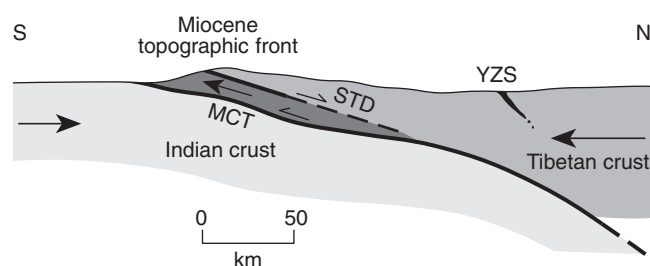


FIGURE 21.2.8 Diagrammatic cross section through the Himalayas and southern Tibet showing the southward ejection of a crustal wedge bounded below by the MCT and above by the South Tibetan Detachment (STD). Near Qomolangma (Mt. Everest) both faults were active at about 20 Ma, during the convergence of India. Faulting is thought to be due to gravitational collapse of the Miocene topographic front. The geometry shown at depth is speculative. YZS is the Indus-Tsangpo suture zone.

and represents a crucial point in developing new models for the deformation of the plateau. It is perhaps noteworthy that the grabens occur mainly in the western two-thirds of the plateau and that some of the grabens extend southward through the Himalaya and nearly to the Himalayan thrust front.

Within the High Himalaya there is also evidence for large-scale north-south extension that preceded the younger east-west extension and occurred on gently north-dipping normal faults (the South Tibetan Detachment zone) that parallel the MCT (Figure 21.2.3) and form a major structural break between the crystalline rocks of the High Himalaya and the rocks of the Tibetan Sedimentary Zone (Figure 21.2.3). Extension occurred simultaneously with thrusting on the Main Central Thrust zone, as indicated by dates of 20 Ma on both fault systems near Qomolangma (Mt. Everest). The normal fault zone juxtaposes rocks of mid-crustal levels in the footwall against shallow-level sedimentary rocks in the hanging wall, and has a minimum displacement of 40 km (although the total displacement could be much greater). A north-south cross section through the fault shows that it bounds the top of a mid-crustal wedge that was ejected southward at about 20 Ma (Figure 21.2.8). This wedge was bounded at its base by the Main Central Thrust zone. Southward ejection of the wedge was from an area of high topography to an area of low topography and probably reflects gravitational collapse of the steep topographic slope along the southern margin of the Tibetan Plateau. Collapse may have occurred due to weakening of the crust by melting of granites at mid-crustal depths, as suggested by the presence of ductilely deformed synkinematic granites along and just below the South Tibetan

Detachment Fault. Several other areas within Tibet contain low-angle faults with normal displacement, but at present they are only recognized on short fault segments and their regional significance remains uncertain.

The occurrence of north-south extension of large magnitude along the southern margin of the plateau is somewhat surprising, since extension was not only contemporaneous with north-south shortening along the MCT but also occurred during continued north-south convergence of India and Eurasia at about 50 mm/y. This indicates that the extensional processes that controlled deformation within the mid- to upper crust in this region were essentially decoupled from the convergent motions occurring deeper in the crust and within the mantle lithosphere. It is probable that the mid- to upper crustal deformation under many, if not all, parts of the plateau is decoupled from the lower crust and mantle. For example, the general style of deformation within the thrust belts that rim the northern and northeastern margins of the plateau, and in some cases balanced cross sections constructed across the thrust belts, show that the thrust faults sole out at depths of about 15 km. Moreover, the relationship of the large strike-slip faults (such as the Haiyuan Fault) within the plateau to adjacent thrust-fault systems also indicates that many of the strike-slip faults are probably restricted to upper and mid-crustal depths (Figure 21.2.7). Thus the motions of crustal fragments within the plateau and along the margins of the plateau may not reflect the motion or deformation of the underlying lower crust and uppermost mantle.

21.2.6 Closing Remarks

Many fundamental questions remain to be answered within the Himalayan-Tibetan region. Some of these appear straightforward, but addressing them will require many years of intensive field work. For instance, how is active crustal deformation partitioned within the plateau? How can we unravel the active and young deformation of the plateau to learn about the pre-Pliocene history of the plateau and its growth through time? Finding the answers to these and other questions will require the use of sophisticated geophysical techniques in combination with field geologic data; for example, how is the deformation partitioned vertically within the crust of the Tibetan plateau? How is crustal deformation related to motions within the underlying mantle? On what length scale is crustal deformation related to motions within the mantle? On the scale of the plate boundary system as a whole (a region 1000 by 2000 km²) it is likely that the averaged motions of the

upper crust and the mantle lithosphere are reasonably similar. Is this also true at smaller scales, such as over regions a few hundreds of kilometers in length and width? How do we go about determining the degree of coupling between the crust and the mantle?

Lastly, one of the most controversial issues surrounding the geologic evolution of the Tibetan Plateau is the history of uplift of the plateau surface to its present elevation of about 5000 m. This is important not only to geologists, because it bears on the mechanisms by which the plateau has been deformed, but also to a wide range of scientists in fields from marine geology to climate modeling. Because the Tibetan Plateau is so large and stands so far above sea level, its uplift is thought to have influenced global circulation patterns within the atmosphere and to have been responsible for the onset of the Indian monsoons, which did not exist prior to Late Miocene time. Uplift of the plateau can also be correlated with changes in faunal distributions within the oceans and with huge changes in the isotopic ratios of elements such as strontium within the worldwide oceans. Indeed, the record of plateau uplift and erosion, as preserved within the composition of marine sediments found worldwide, as well as the geologic record from the plateau itself, suggests that collisional events of the magnitude found in Tibet and the Himalaya are probably rare events, even on a geologic timescale, and that collisional events of comparable magnitude may not have occurred within the last 600 my.

ADDITIONAL READING

- Argand, E., 1977. *Tectonics of Asia* (translation by A. V. Carozzi). Hafner Press: New York.
- Burchfiel, B. C., and Royden, L. H., 1991. Tectonics of Asia 50 years after the death of Emile Argand. *Eclogae Geologicae Helvetica*, 84, 599–629.
- England, P. C., and Houseman, G. A., 1988. The mechanics of the Tibetan Plateau. In Shackleton, R. M., Dewey, J. F., and Windley, B. F., eds., *Tectonic evolution of the Himalayas and Tibet. Philosophical Transactions of the Royal Society of London (A)*, 327, 379–420.
- Lyon-Caen, H., and Molnar, P., 1985. Gravity anomalies, flexure of the Indian plate, and the structure, support, and evolution of the Himalaya and Ganga Basin. *Tectonics*, 4, 513–538.
- Molnar, P., and Tapponnier, P., 1975. Cenozoic tectonics of Asia; effects of a continental collision. *Science*, 189, 419–426.

Molnar, P., 1988. A review of geophysical constraints on the deep structure of the Tibetan Plateau, the Himalaya, and the Karakorum, and their tectonic implications. In Shackleton, R. M., Dewey, J. F., and Windley, B. F., eds., *Tectonic Evolution of the*

Himalayas and Tibet. Philosophical Transactions of the Royal Society of London (A), 326, 33–88.

Tapponnier, P., Peltzer, G., Le Bail, A. Y., Armijo, R., and Cobbold, P., 1982. Propagating extrusion tectonics in Asia: new insight from simple experiments with plasticine. *Geology*, 10, 611–616.

21.3 TECTONICS OF THE ALTAIDS: AN EXAMPLE OF A TURKIC-TYPE OROGEN—An essay by A. M. Celal Őengr¹ and Boris A. Natal'in²

21.3.1 Introduction	535	21.3.4 Implications for Continental Growth	545
21.3.2 The Present Structure of the Altaids	538	21.3.5 Closing Remarks	545
21.3.3 Evolution of the Altaids	539	Additional Reading	545

21.3.1 Introduction

What would happen, if one were to double the entire North American Cordillera back onto itself? Or if one were to collide it with the eastern margin of Asia? Or if the North American Cordillera collided with an orogenic belt similar to itself? In all three cases, one would get a wide orogenic belt, with an extremely complicated interior consisting dominantly of rock types and structures similar to those encountered today along the convergent continental margins of North America and Asia and also along the continental strike-slip margins such as those in California, British Columbia, and the Komandorsky (Bering) Islands. Such an interior would thus be dominated by turbidites deposited in abyssal basins, trenches, and marginal basins; less abundant pelagic deposits (ribbon cherts, pelagic mudstones, some pelagic limestones); local, unconformable shallow water deposits, possibly including coral reefs, lagoonal deposits, local coarse clastic sedimentary rocks; and much volcanogenic material. All of these would appear multiply and highly deformed, tectonically intercalated with diverse rock types making up the oceanic crust and upper mantle (pillow basalts, massive diabases, gabbros, cumulate and/or massive tectonized ultramafic rocks forming the members of the ophiolite suite), and intruded by calc-alkalic plutons ranging from gabbros to granodiorites. Why would this be so? Much of the ensemble described above would be covered by the volcanic equivalents of the calc-alkalic plutonic rocks, from tholeiitic basalts to andesites, and even to local rhyolites as well as wide blankets of welded tuffs. The structural picture of the ensemble would be bewilderingly complex and would include many episodes of

folding, thrusting with inconsistent (but mainly oceanward) vergence, orogen-parallel to subparallel strike-slip faulting, and even some normal faulting, alternating in time and space. Both the rock types and the structures within the internal part of such an orogen would display longitudinal discontinuity over tens to hundreds of kilometers. By contrast, the outer margins of the orogen would be marked by regular, laterally persistent (on scales of hundreds to thousands of kilometers) fold-and-thrust belts made up dominantly of shelf and epicontinental strata with dominant vergence away from the orogen.

How does such an orogen differ from other collisional orogens such as the Alps and the Himalaya? Simply in the collective width of the scrunched-up oceanic remnants between the colliding continental jaws, the amount of subduction-related magmatic rocks, and the magnitude and frequency of incidence of orogen parallel to subparallel strike-slip motion during orogeny. Both in the Alps and in the Himalaya, the width of oceanic offscrapings never exceeds a few kilometers at most; generally they are much narrower (a few hundreds of meters), in places reducing to nothing, where the original opposing continental jaws come into contact. Associated magmatic arcs usually display a single magmatic axis whose wandering across the strike in time hardly exceeds a few tens of kilometers. In some small collisional orogens, such as the Alps, the magmatic arcs are so very poorly developed as to invite suspicion of whether they ever existed.

The **Altaids** were named by the Austrian geologist Eduard Suess, after the Altay Mountains in Central Asia, shared by Russia, Mongolia, and China. The large, mainly Paleozoic orogenic complex dominates much of central Asia and extends to the Arctic in the west and to the Pacific in the east. Its tectonic units are homologous to those occupying across-strike widths of a few hundred meters in the Himalaya and

¹Istanbul Technical University, Istanbul, Turkey.

²Russian Academy of Sciences, Khabarovsk, Russia.

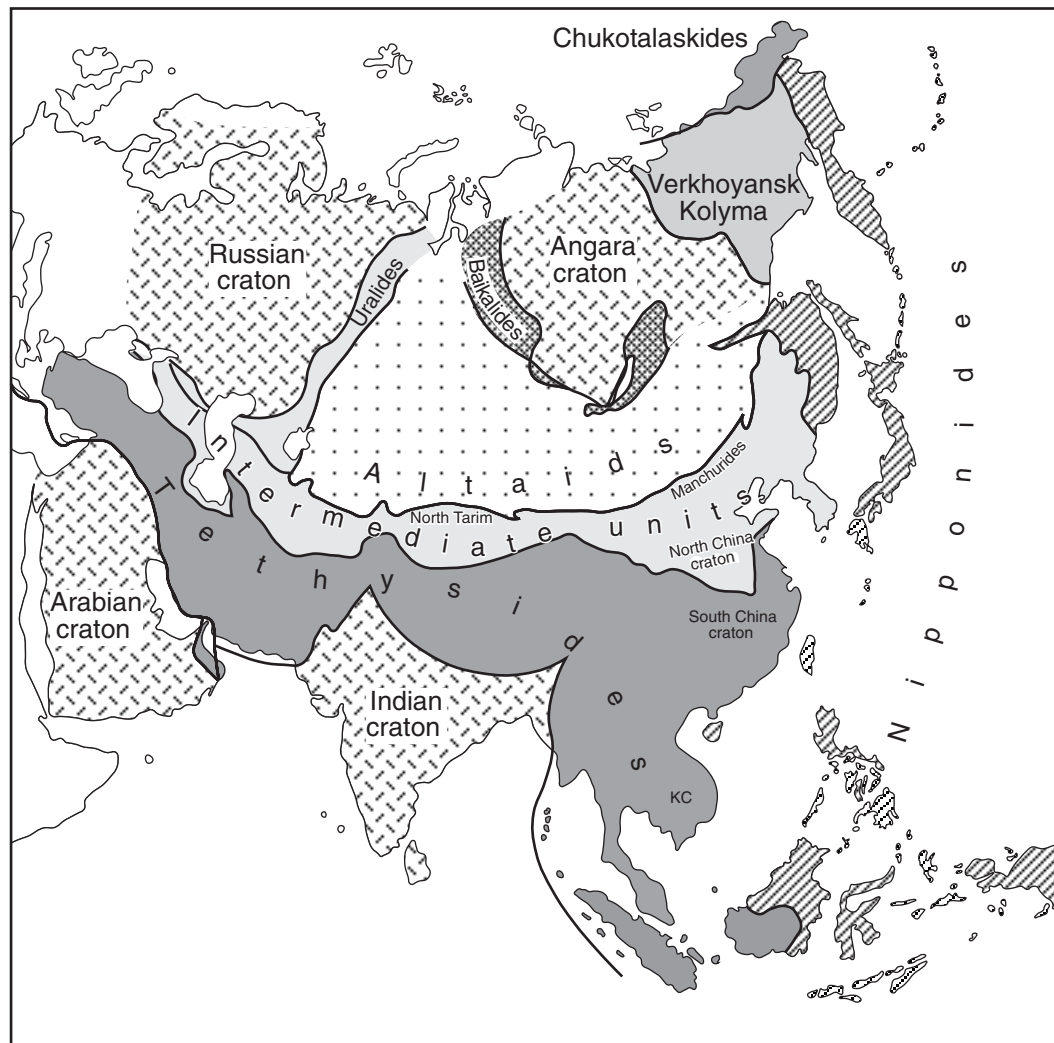


FIGURE 21.3.1 [a] Major tectonic subdivisions of Asia, showing the position of the Altai within the structure of the continent. [b] Tectonic map of the Altai and surrounding large-scale tectonic entities, showing their first-order tectonic units. The Baykalide and the pre-Uralide orogenic systems are not further subdivided. Numbers on the Altai units correspond with the numbers cited for those units in the text.

the Alps but occupy widths of 1500 to 2000 kilometers (Figure 21.3.1). In the North American Cordillera, the edge of the Precambrian crystalline basement is taken to be roughly along the $Sr_1 = 0.704$ line. This line delimits a band, about a 500 km wide and parallel to the coast, north of central California. If one juxtaposes the North American Cordillera against its mirror image, one obtains a band of “off-scraped oceanic material” about 1000 kilometers wide. This is comparable to the width of the internal parts of the Altai, when one considers that the Altai evolution lasted some 50 to 100 my longer than the Cordilleran evolution. Similarly, both in the Altai and in the North American Cordillera, one finds that magmatic axes wandered over distances on

the order of 1000 km. In fact, if we bend the latter collisional orogen approximately 90° about a vertical axis, the picture we obtain is remarkably similar to that of the Altai.

The term Turkic-type has been applied to collisional orogens resulting from the collision of continents that began with very wide subduction-accretion material, long-lasting subduction and rich sedimentary material fed into trenches. These orogens are named after the dominant ethnic group that has populated, in much of known history, the area of development of their best example, namely the Altai. The purpose of this chapter is to present a synopsis of both the present structure and the history of evolution of the Altai, which are an example of a Turkic-type development.

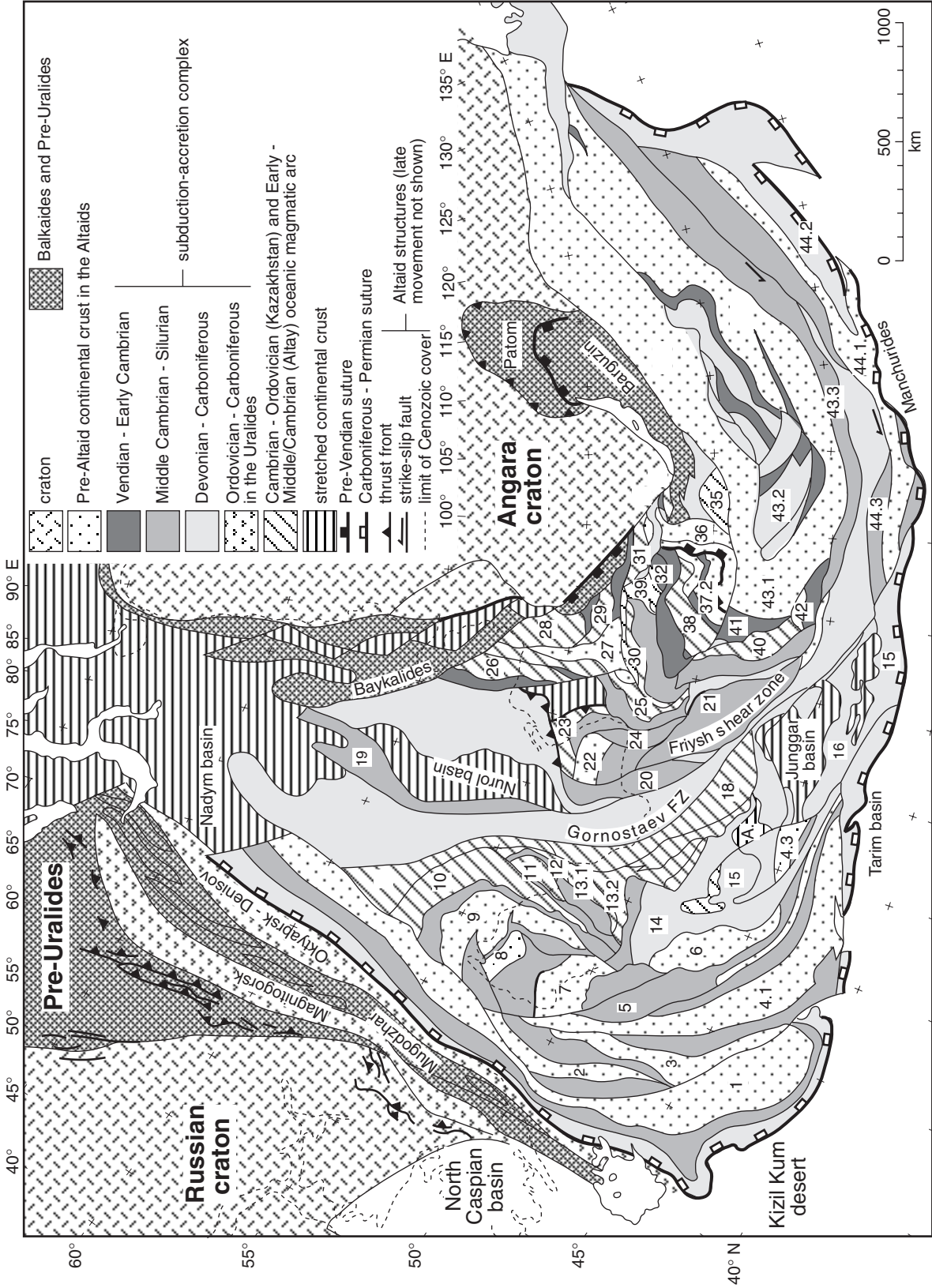


FIGURE 21.3.1 (Continued)

21.3.2 The Present Structure of the Altaids

In Figure 21.3.1a we see the Altaids within the context of the structure of Asia, while Figure 21.3.1b is a tectonic map of the Altaids. Only four main types of genetic entities are displayed in Figure 21.3.1. They are (1) units made up of continental crust that had already formed before the Altaid evolution commenced, (2) subduction-accretion complexes formed during the Altaid evolution, (3) ensimatic magmatic arc massifs formed during the Altaid evolution, and (4) continental crust (of any age) stretched and thinned as a consequence of Altaid evolution. These genetic entities are grouped into 44 main tectonic units defined on the basis of their function during the Altaid evolution, and include units such as arcs, cratons, passive continental margins, and the like. In the following list we briefly characterize their function; more detailed characterization and a summary of the rock content can be found in the readings at the end of this essay. The numbers of the units in the list correspond with the numbers shown in Figure 21.3.1.

1. *Valerianov-Chatkal unit*: Pre-Altaid continental crust, Paleozoic accretionary complex and magmatic arc.
2. *Turgay unit*: Pre-Altaid continental crust, Altaid accretionary complex and magmatic arc; all buried under later sedimentary cover.
3. *Baykonur-Talas unit*: Pre-Altaid continental crust, Early Paleozoic magmatic and arc accretionary complex.
- 4.1. *Djezkazgan-Kirgiz unit*: Pre-Altaid continental crust, Paleozoic accretionary complex and magmatic arc.
- 4.2. *Jalair-Nayman unit*: Pre-Altaid continental crust, Early Paleozoic marginal basin remnants, Early Paleozoic magmatic arc and accretionary complex.
- 4.3. *Borotala unit*: Pre-Altaid continental crust, Early Paleozoic magmatic arc and accretionary complex.
5. *Sarysu unit*: Paleozoic accretionary complex and magmatic arc.
6. *Atasu-Mointy unit*: Pre-Altaid continental crust, Early Paleozoic (including the Silurian) magmatic arc and accretionary complex.
7. *Tengiz unit*: Pre-Altaid continental crust, Vendian-Early Paleozoic magmatic arc and accretionary complex.
8. *Kalmyk Köl-Kökchetav unit*: Pre-Altaid continental crust, Vendian-Early Paleozoic magmatic arc and accretionary complex.
9. *Ishim-Stepnyak unit*: Pre-Altaid continental crust, Vendian-Early Paleozoic magmatic arc and accretionary complex.
10. *Ishkeolmes unit*: Early Paleozoic ensimatic magmatic arc and accretionary complex.
11. *Selety unit*: Early Paleozoic ensimatic magmatic arc and accretionary complex, with questionable pre-Altaid continental basement in fault contact.
12. *Akdym unit*: Vendian(?) and Early Paleozoic ensimatic magmatic arc and accretionary complex.
13. *Boshchekul-Tarbagatay unit*: Early Paleozoic (including the Silurian) ensimatic magmatic arc and accretionary complex.
14. *Tekturmas unit*: Ordovician-Middle Paleozoic accretionary complex, Middle Devonian-Early Carboniferous magmatic arc.
15. and 16. *Junggar-Balkhash unit*: Early (ensimatic) through Late (ensialic) Paleozoic magmatic arc, Middle through Late Paleozoic accretionary complex.
17. *Tar-Muromtsev unit*: Early Paleozoic ensimatic magmatic arc and accretionary complex.
18. *Zharma-Saur unit*: Early to Late Paleozoic ensimatic magmatic arc, Early Palaeozoic accretionary complex.
19. *Ob-Zaisan-Surgut unit*: Late Devonian-Early Carboniferous accretionary complex, strike-slip fault-bounded fragments of the Late Devonian-Early Carboniferous arc, Late Paleozoic magmatic arc.
20. *Kolyvan-Rudny Altay unit*: Early and Middle-Late Paleozoic magmatic arc.
21. *Gorny Altay unit*: Early Paleozoic magmatic arc and accretionary wedge, superimposed by Middle Palaeozoic magmatic arc; farther west in the "South Altay," Middle Paleozoic accretionary complex with forearc basin.
22. *Charysh-Chuya-Barnaul unit*: Pre-Altaid continental crust, Early Paleozoic magmatic arc and accretionary complex, and Middle Paleozoic magmatic arc and forearc basin.
23. *Salair-Kuzbas unit*: Pre-Altaid continental crust, Vendian-Early Paleozoic magmatic arc and accretionary complex, Ordovician-Silurian forearc basin, Devonian pull-apart basin, Late Palaeozoic foredeep.
24. *Anuy-Chuya unit*: Early Paleozoic magmatic arc and accretionary complex.

25. *Eastern Altay unit*: Pre-Altai continental crust, Early Paleozoic magmatic arc and accretionary complex.
26. *Kozykhov unit*: Early Paleozoic magmatic arc and accretionary complex.
27. *Kuznetskii Alatau unit*: Pre-Altai continental crust, Early Paleozoic magmatic arc and accretionary complex.
28. *Belyk unit*: Vendian-Middle Cambrian magmatic arc and accretionary complex.
29. *Kizir-Kazyr unit*: Vendian-Middle Cambrian magmatic arc and accretionary complex.
30. *North Sayan unit*: Vendian-Early Paleozoic magmatic arc and accretionary complex.
31. *Utkhum-Ota unit*: Pre-Altai continental crust, Early Paleozoic magmatic arc and accretionary complex.
32. *Ulugoi unit*: Vendian-Early Cambrian magmatic arc and accretionary complex.
33. *Gargan unit*: Pre-Altai continental crust, Early Paleozoic magmatic arc, Vendian-Early Paleozoic accretionary complex.
34. *Kitoy unit*: Early Paleozoic magmatic arc.
35. *Dzida unit*: Early Paleozoic magmatic arc and accretionary complex.
36. *Darkhat unit*: Pre-Baikalide continental crust, Riphean magmatic arc and accretionary complex.
37. *Sangilen unit*: Baikalide microcontinent that collided in the Riphean with the Darkhat unit (unit 36) and the Tuva-Mongol Massif (see unit 43.1) and experienced dextral strike-slip displacement during the early Altai evolution.
38. *Eastern Tannuola unit*: Early Paleozoic magmatic arc and accretionary complex.
39. *Western Sayan unit*: Early Paleozoic magmatic arc and accretionary complex.
40. *Kobdin unit*: Early and Middle Paleozoic magmatic arc and accretionary complex.
41. *Ozernaya unit*: Vendian-Early Cambrian magmatic arc and accretionary complex.
42. *Han-Taishir unit*: Pre-Altai continental crust, Vendian-Early Cambrian magmatic arc and accretionary complex.
43. *Tuva-Mongol unit*:
 - 43.1. *Tuva-Mongol arc massif*: Pre-Altai continental crust and Vendian-Permian magmatic arc.
 - 43.2. *Khangay-Khantey unit*: Vendian-Triassic accretionary complex.
 - 43.3. *South Mongolian unit*: Ordovician to Early Carboniferous accretionary complex.

44. *South Gobi unit*: Pre-Altai continental crust, Paleozoic magmatic arc, Early and Late Paleozoic accretionary complex.

21.3.3 Evolution of the Altai

METHOD OF RECONSTRUCTION The problem with the Altai has long been how to establish the trend-line of the orogen amidst the abundance of the variably oriented tectonic units listed in the preceding section. Since the late 1800s, the trend-lines of orogenic belts have been depicted as the direction, in any given cross section, of the average strike, particularly in the laterally persistent external fold-and-thrust belts. That approach worked well for narrow, linear, and/or arcuate orogens such as the Alpine system and even the Cordillera, but the strange map shape of the Altai makes such an approach suspect. The median line of an orogen along its internal parts, consisting of median masses (Zwischengebirge) and the so-called scar-lines (Narbe), has also been used to follow the orogenic trend-line, but if one tried that method on the Altai, the trend-line obtained from the external belts and the trend of the median line would give two different, contradictory results. Try to confirm this for yourselves by using Figure 21.3.1b. So, that approach will not be satisfactory either.

The difficulty of identifying the trend-line of the orogenic edifice in the Altai has led to proposals that they might consist of more than one independent orogenic belt. However, the great similarity of the rock material involved in their architecture, the significant uniformity of style of their internal structure, the broad correspondences between their disparate sectors in timing of tectonic evolution, and the difficulty of finding “junctures” where one orogen would join another one, make it unlikely that there are a number of independent orogenic belts tucked away within the Altai realm.

It has been proposed that *magmatic fronts of arcs* constitute convenient markers to follow the orogenic trend owing to their easy identification, lateral persistence, and indication of facing; they are very sharp on the ocean side (i.e., the side toward which they are said to “face”), but more diffuse on the backarc side. This idea was applied to the entire Altai to trace the first-order trend-lines of the orogen, and it was possible to show that the chaotic internal structure could be interpreted in terms of the deformation of formerly simpler arc geometries.

In Figure 21.3.2 we see how this idea is applied to the western and central sector of the Altai (the

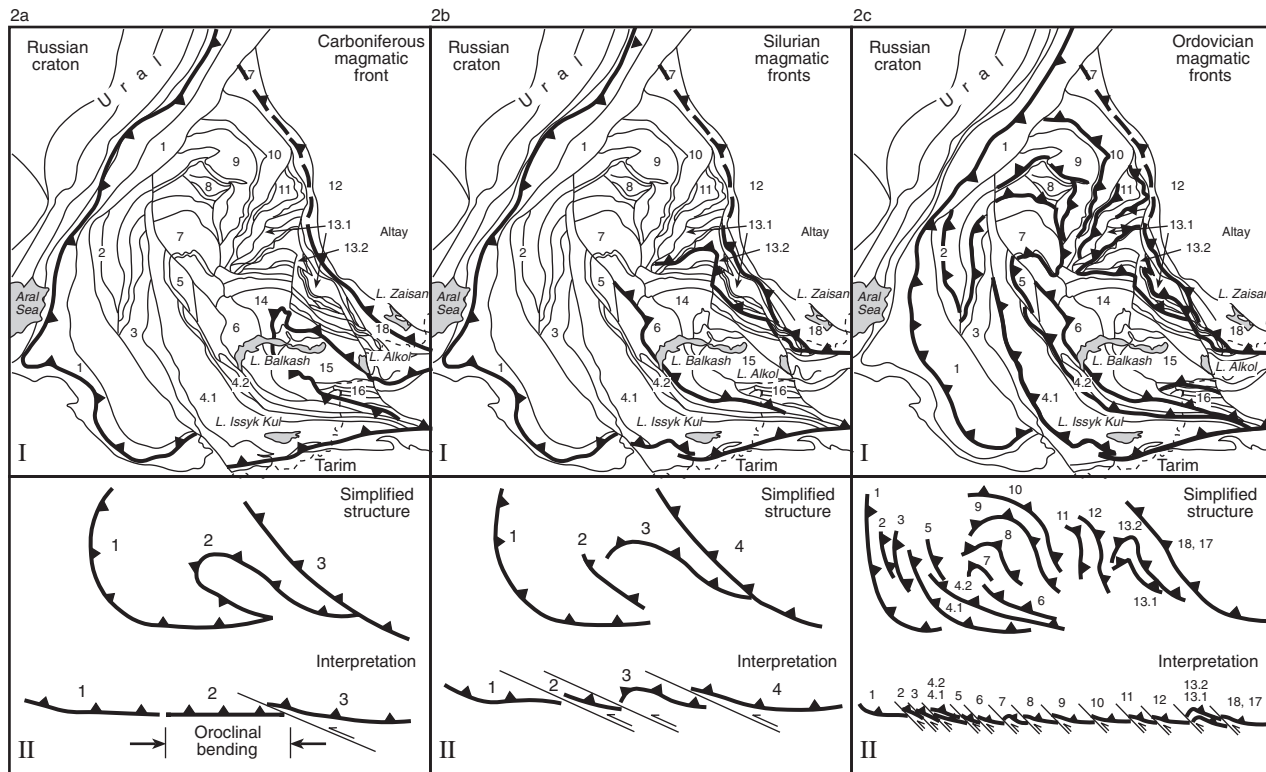


FIGURE 21.3.2 (a) Carboniferous magmatic fronts (I) and their schematic palinspastic interpretation (II). Magmatic fronts are shown with thrust symbols, and face in the opposite direction from the apices of the triangles. The numbers in I correspond to the unit identifications in Figure 21.3.1b and in the reconstructions displayed in Figure 21.3.4. In II, the numbers 1, 2, and 3 correspond to the Valerianov/Tien Shan, the central Kazakhstan, and the Zharma-Saur fronts, respectively. In II, the figure on top is a highly schematized version of the present geometry of the Carboniferous magmatic fronts, as shown in I; the bottom figure is an interpretation of the top configuration in terms of a former single arc. (b) Silurian magmatic fronts (I) and their schematic palinspastic interpretation (II). The numbers in I correspond to the unit identifications in Figure 21.3.1b and in the reconstructions displayed in Figure 21.3.4. In II, the numbers 1, 2, 3, and 4 correspond to the Valerianov/Tien Shan, the Atasu-Mointy, the central Kazakhstan, and the Zharma-Saur fronts, respectively. In II, the figure on top is a highly schematized version of the present geometry of the Silurian magmatic fronts, as shown in I; the bottom figure is an interpretation of the top configuration in terms of a former single arc. (c) Ordovician magmatic fronts (I) and their schematic palinspastic interpretation (II). The numbers in I correspond to the unit identifications in Figure 21.3.1 and in the reconstructions displayed in Figure 21.3.4. In II, the magmatic fronts can be grouped into three domains: fronts 1–6, the Tien Shan–southwest Kazakhstan domain; fronts 7–13, north-central Kazakhstan; and fronts 17 and 18, the Zharma-Saur domain. Here the enumeration of the magmatic fronts corresponds with the unit numbers in Figure 21.3.1b. In II, the figure on top is a highly schematized version of the present geometry of the Ordovician magmatic fronts, as shown in I. The bottom figure is an interpretation of the top configuration in terms of a former single arc.

Kazakhstan-Tien Shan sector). In Figure 21.3.2a, the locations of the Carboniferous magmatic fronts are shown (I). Note that, with the exception of the central Kazakhstan front, they exist only on the outer periphery of the ensemble of tectonic units and pass from one unit to another. This indicates that, by the Carboniferous, the units making up the western and central sector of the Altaids had already come together (because the magmatic front “stitches” the outer units together). Panel II shows how this picture may be interpreted in terms of a single arc. At the top of Panel II a simplified trend-line pattern is shown, which corresponds with the actual geometry in Panel I. At the bottom of Panel II, this is interpreted in terms of strike-slip disruption of a formerly continuous front. Figure 21.3.2b shows the magmatic fronts of the Silurian. In general they are not dissimilar to those in the Carboniferous, but they show a marked difference in detail. The fronts have migrated inwards along the outer periphery, whereas in central Kazakhstan they moved outward, and the front along units 5 and 6 has changed its polarity. Note how these changes affect the interpretation. Figure 21.3.2c I exhibits a much greater complication and we no longer see the neat picture of the earlier frames. As seen in Panel II, the

interpretation is correspondingly more complicated. (Can you tell wherein lies the complication?)

The magmatic fronts in the Altaids may thus be interpreted in terms of a single arc. But was it really so? In other words, does this agree with the rest of their geology? In order to check that we must find tie-points (i.e., points that are now far away from one another, but that used to be adjacent to one another) on adjacent units that would allow us to bring them back to their pre-faulting positions. This is not a straightforward exercise, because many geologic features can be used as tie-points. This analysis uses the arc massif-accretionary complex contacts as one set of tie-points. Faulted and displaced forearc basin parts, segments of backarc basins, and metamorphic complexes are among other features that have been used as features providing tie-point sets for reconstructions in the Altaids.

In Figure 21.3.3 we see the disassembled units in the Kazakhstan-Tien Shan sector of the Altaids, with an emphasis on the arc massif-accretionary complex contacts. The reconstructed single arc at the bottom of the figure is generated by bringing into juxtaposition the tie-points on adjacent units. Thus, much of the Altaid edifice could be interpreted as the deformed remnants of a single magmatic arc, called the Kipchak

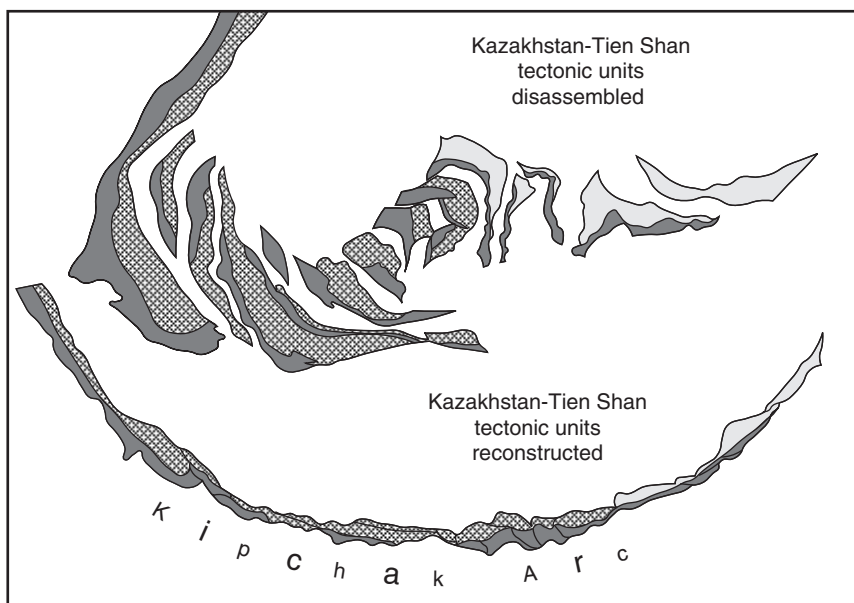


FIGURE 21.3.3 Method used in the reconstruction of the Kipchak arc. At the top is a “disassembled” version of the Kazakhstan–Tien Shan sector of the Altaid orogenic collage. These units were then reconstructed into the Kipchak arc by using tie-points. These tie-points represent points on correlative accretionary complex–backstop contacts. The reconstruction is then checked against those made by correlating magmatic fronts [shown in Figure 21.3.2]. While doing our reconstructions, we also used other sorts of tie-points, correlating such features as forearc basins, metamorphic complexes, and backarc basin sutures, but they are not shown here to maintain legibility.

arc (after the dominant ethnic group inhabiting the area where its fragments are now found), now disrupted and squeezed between the two cratons of Russia and Angara. Altaids extending eastwards into Mongolia evolved from a second arc (Tuva-Mongol) as shown in the reconstructions in Figure 21.3.4. (Can you find this second arc in Figure 21.3.1?)

The location of the two arcs with respect to the two continental nuclei of Russia and Angara in the geologic past is established by finding a part of the arc that has remained attached to Angara (in the case of the Kipchak arc, in the vicinity of the southern tip of Lake Baykal; in the case of the Tuva-Mongol Arc, in the Stanovoy Mountains along the Stanovoy Fault; see Figure 21.3.1), and then comparing the geology to that of the margins of the Angara and the Russian cratons. Ideally one would like to support this procedure with paleomagnetic data to check paleolatitudes and paleorientations of the individual Altaid units, but, in the case of the Altaids,

reliable paleomagnetic data are very scarce. Only the positions of the two major cratons are known with any degree of confidence (Russia being better known than Angara). Figure 21.3.4 shows the result of such geologic comparisons.

First-Order Tectonic Evolution of the Altaids

In Figure 21.3.4a we show the picture obtained by reconstructing the positions of the two major cratons of Angara and Russia in the Vendian (~630–530 Ma), and placing the Kipchak and the Tuva-Mongol arcs onto the resulting large continent. Rifting in the Vendian left fields of dykes and normal-fault-bounded basins both to the north of Angara and Russia. As the two began to separate from each other, the Kipchak arc also detached itself (as shown in Figure 21.3.4b; Early Cambrian, ~547–530 Ma) in front of an opening marginal basin (the future Khanty-Mansy Ocean³) that may have been as large as the present Philippine Sea or the Tasman Sea, both of which also opened as backarc basins behind migratory arcs.

Units 10–18 have been formed by **ensimatic** arcs that may have nucleated along a long transform fault that connected the Kipchak subduction zone with the Tuva-Mongol subduction zone. That transform fault must have met the Kipchak arc at a triple junction as shown, otherwise the kinematics does not make sense. Can you guess why? By Late Cambrian time (~514 Ma) the triple junction migrated along the Kipchak arc, and the former transform fault turned into a subduction zone nucleating magmatic arcs along itself, thus lengthening the Kipchak arc. West-dipping subduction also started below the future Urals along the eastern margin of the present-day Mugodzhar unit, an **ensialic** magmatic arc remnant in the southern and central Urals.

Transpression along the outer Tuva-Mongol subduction zone had begun slicing up the active margin and transporting arc and accretionary complex fragments towards the Angara craton. By contrast, along the inner margin, facing the Khangai-Khantey Ocean, the geometry of subduction was much simpler. It is now impossible to reconstruct palinspastically the Tuva-Mongol fragment itself.

In the Middle Ordovician (~458 Ma) the same picture as in the Late Cambrian seems to persist (Figure 21.3.4c), except that in two places along the

Kipchak arc, marginal basins (Boschekul-Tarbagatay and Djezkazgan-Kirgiz-Jalair-Nayman) resembling the present-day West Mariana Basin in position, but the Japan Sea in tectonic character, began to open. (Can you guess why they were similar to the West Mariana Basin in position, but to the Japan Sea in tectonic character?) Also rifting began tearing away a strip of land from Russia that eventually formed the Mugodzhar microcontinental arc in front of the opening marginal basin of Sakmara-Magnitogorsk in the southern and central Urals.

By Late Ordovician time, the two major cratons of Angara and Russia had rotated sufficiently towards each other and began squeezing the oceanic space between them, spanned by the Kipchak arc. This resulted in the collision of the tip of the arc with the Mugodzhar arc, similar to the collision of the Izu-Bonin arc with the Japan arc today. Further shortening led to the internal deformation of the Kipchak arc that was expressed by cutting up the arc by strike-slip faults (perhaps similar to the Philippines Fault cutting the Philippine island arc system today) and stacking its pieces beside each other along the strike-slip faults. The resulting geometry resembles thrust stacks tipped on their side.

In the Middle Silurian (about 433 Ma), the Kipchak arc broke along a left-lateral transform fault system, bounding units 5, 6 and 7, 8. In the Early Devonian (~390 Ma; Figure 21.3.4d), the transform fault became lengthened and its southern parts turned compressional. A substantial microcontinent had thus become assembled in the middle parts of the arc by the previous stacking. In the north, the eastern part of the Tuva-Mongol fragment collapsed onto the Sayan Mountains. From now on, strike-slip transfer of units along the Tuva-Mongol fragment passed directly onto the future site of the Altay Mountains.

The Late Devonian (~363 Ma) witnessed much the same sort of evolution as in the Early Devonian, except that at this time, the Angara craton began a right-lateral shear motion with respect to the Russian craton. Various backarc and pull-apart basins opened in the continuously deforming stacked Kipchak arc ensemble and this deformation began tightening the Kazakhstan orocline. Newer units were continuously being fed into the Altay from the coastwise transport along the Tuva-Mongol fragment (not unlike the Cordilleran System, especially in Canada and Alaska in the Mesozoic and Cenozoic). This further narrowed the deep gulf within the Kazakhstan orocline into which rich turbidite deposits were being fed from the surrounding mountainous frame. This was also the time in which the Sakmara-Magnitogorsk marginal basin reached its

³The name Khanty-Mansy is another name derived from the aboriginal local populations living in the northern part of the Western Siberian Lowlands.

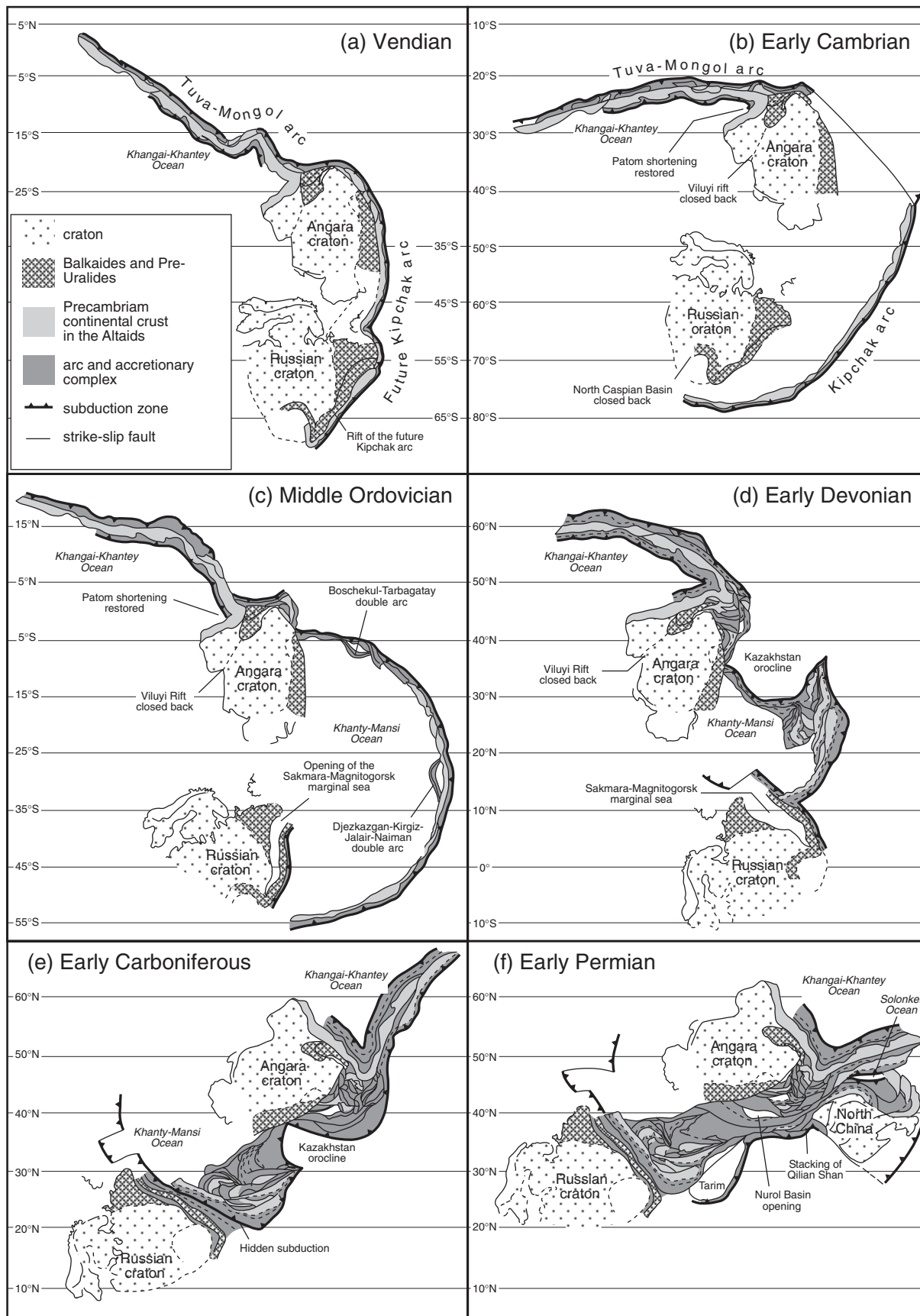


FIGURE 21.3.4 Reconstructions of the Altaids. (a) Vendian reconstruction (~630–530 Ma). The legend shown here applies to all reconstructions shown in Figure 21.3.4. (b) Early Cambrian reconstruction (~547–530 Ma). (c) Middle Ordovician reconstruction (~458 Ma). (d) Early Devonian reconstruction (~390 Ma). (e) Early Carboniferous reconstruction (~342 Ma). (f) Early Permian reconstruction (~270 Ma). The text describes the evolution during intervening times; additional maps and more detailed descriptions are found in the reading list.

apogee and began closing by northward-directed subduction (Late Devonian geographic orientation) under the Mugodzhar arc. It was during the Late Devonian that the North Caspian Basin (pre-Caspian depression in some publications) began opening as a rifted embayment very similar to the Jurassic opening of the Gulf of Mexico. In fact, the present-day Gulf of Mexico is the best analog for the North Caspian Basin.

In the Early Carboniferous (~342 Ma; Figure 21.3.4e), the Sakmara-Magnitogorsk marginal basin was almost completely closed, but because of the continuation of the arc-related magmatism on the Mugodzhar arc, some subduction probably lasted till the end of the Mississippian. To the south of the still-growing Altay Mountains (Early Carboniferous geographic orientation), units 19 (Ob-Zaisan-Surgut) and 20 (Kolyvan-Rudny Altay) were emplaced along the giant Irtysh shear zone into their present locations with respect to the Altay-Sayan Mountain complex. This further narrowed the large embayment within the Kazakhstan orocline, which was rapidly being filled with clastics eroded from the surrounding Altaid units. The right-lateral shear of Angara with respect to the Russian craton continued throughout the Early Carboniferous. In the Late Carboniferous (~306 Ma), the gulf within the Kazakhstan orocline was obliterated by the continued convergence of the Angara craton and the Russian craton. Any further accretion to the remnants of the Kipchak arc was made impossible by the collision, along the present Tien Shan Mountains, of the Tarim block with the assembled Altaid collage between the Angara and the Russian cratons. The nature of the crust underlying the Tarim block is unknown owing to lack of outcrop and paucity of geophysical data. What little is known indicates that it is a strong, old (Late Proterozoic) crust, which may be a trapped oceanic plateau similar to the present-day Ontong-Java now colliding with the Solomon Islands in the southwest Pacific Ocean.

The right-lateral motion of the Angaran craton with respect to the Russian craton and the Kazakh part of the Altaid collage continued in the Early Permian (~270 Ma; Figure 21.3.4f). This motion was being accommodated mostly along two major shear zones, namely the Irtysh and the Gornostaev. The deep Nuroi Basin within the basement of the West Siberian Lowlands, just north of the Kolyvan Ranges north of the Altay Mountains began forming in the Early Permian as a pull-apart structure along the Irtysh shear zone. This was the earliest harbinger of the beginning extension in the West Siberian Lowlands that lasted until the

Middle Jurassic in different places and under different strain regimes. The earlier episodes of this extension especially are directly related to the Altaid evolution and constitute one spectacular example of extensional basins forming atop former orogenic belts, such as the Eocambrian Hormuz salt basins in Arabia following the latest Precambrian Pan-African Orogeny, or the Middle to Late Cenozoic Western Mediterranean and the Late Cenozoic Aegean Basins following the Alpine Orogeny. (Can you think of similar post-orogenic basins within the United States? How do you think they formed?)

In the Late Permian (~250–255 Ma), the right-lateral motion of the Angara craton with respect to the Russian craton and the Kazakh sector of the Altaid collage reversed. The resulting left-lateral motion was largely accommodated along a broad swath of shear zones south of (Late Permian geographic orientation), and including, the Gornostaev shear zone, creating a broad **keirogen** (a deformed belt dominated by strike-slip motion). The late Permian extensional basins of Nadym, Alakol, Junggar, and Turfan opened along this keirogen as pull-apart structures, involving internal counterclockwise rotations exceeding 90° about vertical axes.

In the Kazakhstan-Tien Shan sector, the Late Permian saw the end of the Altaid orogenic evolution, although extension in the West Siberian Lowlands continued until the Early Jurassic, possibly resulting from continued limited jostling of the Angara and the Russian cratons along the large Gornostaev keirogen. Farther east (present geographic orientation), Altaid orogenic evolution continued in the Mongolian-Far Eastern sector by the ongoing closure of the Khangai-Khantey Ocean as a consequence of the collision of the North China block with the South Gobi units (unit 44). The progressive narrowing of the Khangai-Khantey Ocean lasted until the Jurassic. During this narrowing, a part of the accretionary fill, formed by the Kangai-Khantey accretionary complex (unit 43.2), was extruded northwestwards. (Can you guess why?) By Jurassic time, the Mongolia/east Russia/northeast China regions acquired more-or-less their present-day architecture; there was some shortening in the extreme far eastern Russian Altaiids continuing into the early Cretaceous, but by then it was under the influence of the Nipponide evolution (i.e., orogeny resulting from the interaction of oceanic plates in the Pacific Ocean with the eastern margin of Asia) and not an integral part of the Altaid development.

21.3.4 Implications for Continental Growth

The time slices in Figure 21.3.4 show how significant volumes of new continental crust were added to the Altiids edifice as it developed from Vendian times onward. It is estimated that some 10^{12} km³ of material may have been added to the bulk of Asia between the Vendian and the Late Permian (not taking into account the Khangai-Khantey accretionary complex), which accounts for some 40% of the total Paleozoic crustal growth rate. Clearly, the Altiids represent a major tectonic system during Earth's history in the Paleozoic. This accretionary aspect of Turkic-type orogeny may offer insights into the formation of Earth's earliest continental crust, as discussed in the following section.

21.3.5 Closing Remarks

The Altiids are the most spectacular example of a Turkic-type collisional orogen in the Phanerozoic. Turkic-type orogens form by collision of very large, subcontinent-size subduction-accretion complexes fringing two (or more) converging continents and/or island arc systems. Three main processes contribute to the consolidation of such large subduction-accretion complexes into respectable continental basement:

1. Invasion of former forearc regions by arc plutons through the trenchward migration of the magmatic axis as the trench recedes and the subduction-accretion complex becomes wider.
2. Continuing bulk shortening of the subduction-accretion complex.
3. Metamorphism of the accretionary complex up to high-amphibolite grade, either by ridge subduction or by the exposure of its bottom to hot asthenosphere by steepening of the subduction angle.
4. Further thickening of subduction-accretion complexes and melting of their bottoms as a consequence of the convective removal of the lithospheric mantle.

Recognition of Turkic-style orogeny has long been hampered by emphasis on Alpine- and Himalayan-type collisional orogens, which has been conditioned by the familiarity of the world geologic community with the Alps, the Himalaya, the European Hercynides, and the Caledonian/Appalachian mountain ranges. The study of the Altiids and their comparison with the North American Cordillera have begun to uncover the

main features of their architecture and the rules of their development. Many of the familiar features guiding the geologist in Alpine- and Himalayan-type collisional orogens lose their significance in the Turkic-type orogenic systems. Although abundant ophiolitic slivers, nappes, and flakes exist in vast areas occupied by Turkic-type orogens, these do not necessarily mark sites of sutures. Intra-accretionary wedge-thrust faults and, especially, large strike-slip faults, commonly juxtapose assemblages formed in distant regions, and deformed and metamorphosed at different structural levels. Such faults are likely to mislead geologists into thinking that they are sutures, bounding different, originally independent microcontinental "terranes." The recognition of the Turkic-type orogeny has thus made necessary not only detailed and careful field mapping and description, in terms of **genetic labels**, but also detailed geochemical sampling to see how much of the accreted material is juvenile, and how much is recycled.

It is proposed that Turkic-type collisional orogeny was very widespread in the Proterozoic, possibly largely dominated the Archean development, and contributed significantly to the growth of the continental crust through time.

ADDITIONAL READING

- Allen, M. B., Şengör, A. M. C., and Natal'in, B. A. 1995. Junggar, Turfan, and Alakol basins as Late Permian to ?Early Triassic sinistral shear structures in the Altiid orogenic collage, Central Asia. *Journal of the Geological Society of London*, 152, 327–338.
- Burke, K., 1977. Aulacogens and continental breakup. *Annual Review of Earth and Planetary Sciences*, 5, 371–396.
- Kober, L. 1921. *Der Bau der Erde*. Gebrüder Borntraeger: Berlin.
- Şengör, A. M. C., 1990. Plate tectonics and orogenic research after 25 years: a Tethyan perspective. *Earth Science Reviews*, 27, 1–201.
- Şengör, A. M. C., 1991. Plate tectonics and orogenic research after 25 years: synopsis of a Tethyan perspective. *Tectonophysics*, 187, 315–344.
- Şengör, A. M. C., and Natal'in, B. A., 1996a. Palaeotectonics of Asia: fragments of a synthesis. In Yin, A., and Harrison, M., eds., *The tectonic evolution of Asia*, Rubey Colloquium. Cambridge University Press: Cambridge.

- Şengör, A. M. C., and Natal'in, B. A., 1996b. Turkic-type orogeny and its role in the making of the continental crust. *Annual Review of the Earth and Planetary Sciences*, 24, 263–337.
- Şengör, A. M. C., and Okurogullari, A. H., 1991. The role of accretionary wedges in the growth of continents: Asiatic examples from Argand to plate tectonics. *Eclogae Geologicae Helvetiae*, 84, 535–597.
- Şengör, A. M. C., Natal'in, B. A., and Burtman, V. S., 1993. Evolution of the Alaid tectonic collage and Palaeozoic crustal growth in Eurasia. *Nature*, 364, 299–307.
- Stille, H., 1928. Der Stammbaum der Gebirge und Vorlaender: *XIVe Congrès Géologique International (1926, Espagne)*, 4. Fasc., 6. Partie, Sujet XI (Divers), Graficas Reunida S. A., Madrid, 1749–1770.
- Suess, E., 1901[1908], *The face of the Earth (Das Antlitz der Erde)*, v. 3, translated by H. B. C. Sollas under the direction of W. J. Sollas. Clarendon Press: Oxford.

21.4 THE TASMAN OROGENIC BELT, EASTERN AUSTRALIA: AN EXAMPLE OF PALEOZOIC TECTONIC ACCRETION—An essay by David R. Gray¹ and David A. Foster²

21.4.1 Introduction	547	21.4.4 Mechanics of Deformation in Accretionary Orogens	554
21.4.2 Crustal Structure and Main Tectonic Elements	548	Additional Reading	555
21.4.3 Timing of Deformation and Regional Events	551		

21.4.1 Introduction

The **Tasman orogenic belt** is a turbidite-dominated, composite Paleozoic “accretionary” orogenic system along the eastern margin of Australia (Figure 21.4.1). This Paleozoic orogenic system illustrates how deformational and metamorphic processes, combined with magmatism, convert deep-marine sedimentary and volcanic rocks, including large turbidite fan systems, into normal-thickness (~35 km) continental crust. Shortening and accretion occurred by stepwise deformation and metamorphism away from the cratonic core over a period of 400 m.y. from Cambrian through Triassic times. During that time eastern Australia underwent an important period of continental accretion, which added approximately 30% to the size of the ancient Australian cratonic core. The addition of recycled continental detritus in turbidite fans and of juvenile material to Australia represents a continental crustal growth mechanism that was important throughout Earth history. Originally part of a Paleozoic convergent plate margin that stretched around the supercontinent of Gondwana from South America to Australia, the present distribution of orogens and the observed structural patterns are a response to the chang-

¹University of Melbourne, Australia.

²University of Florida, Gainesville, Florida, USA.

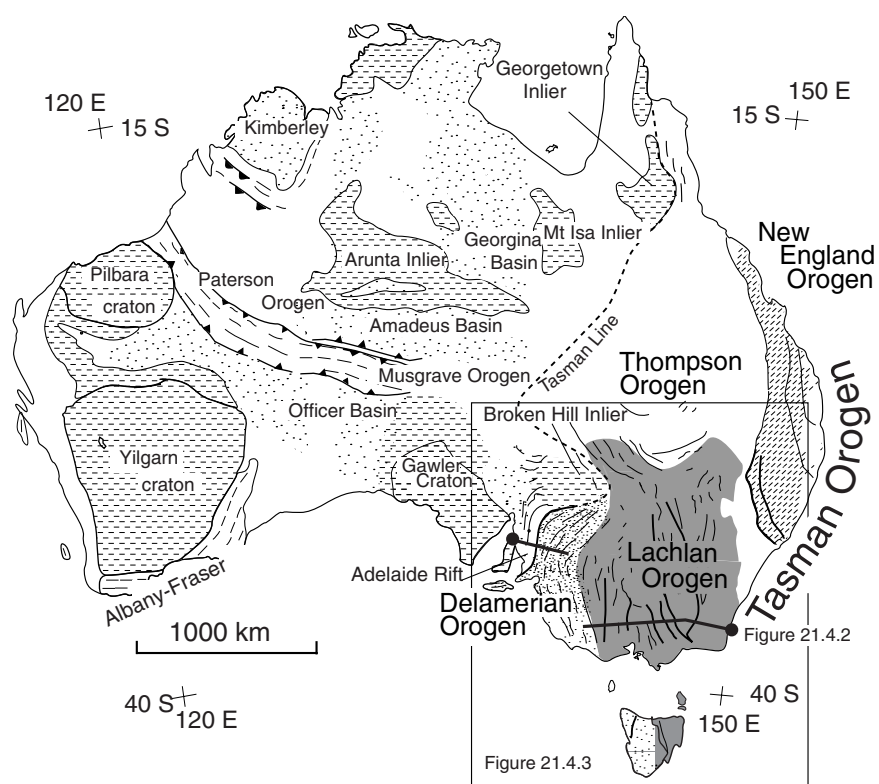


FIGURE 21.4.1 Map of major geologic elements of Australia showing the Tasman Orogen along the eastern margin. Positions of section line (Figure 21.4.2) and the more detailed map area of Figure 21.4.3 are shown.

ing character of the Gondwana margin/plate boundary from the Cambrian to the Triassic.

The features that set the Tasman Orogen apart include:

- The absence of classic sutures that are typical of continental collisional orogenic systems.
- The absence of simple craton-directed thrusting, but juxtaposition of craton-verging and oceanward-verging, marginal thrust systems (Figure 21.4.2).

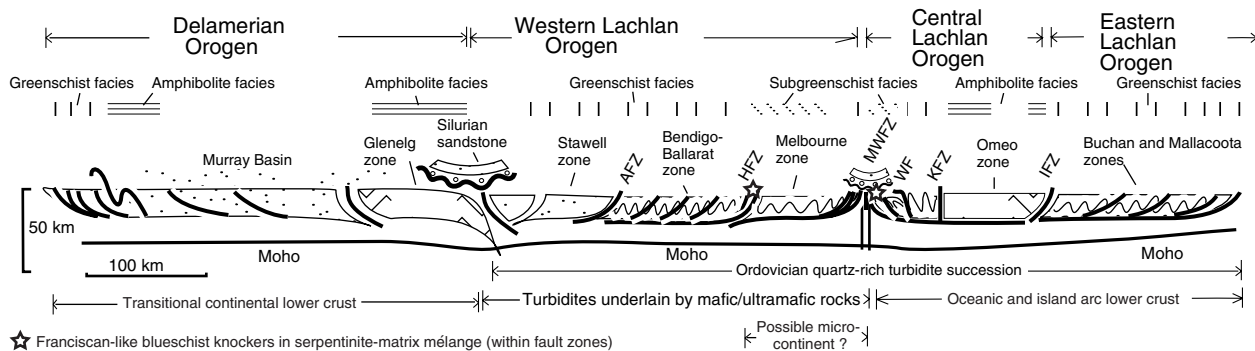


FIGURE 21.4.2 Schematic west-east crustal structural profiles showing the main geologic and metamorphic aspects of the Lachlan Orogen at 37°S latitude. Abbreviations: AFZ-Avoca fault zone, HFZ-Heathcote fault zone, MWFZ-Mt Wellington fault zone, WF-Wonnangatta Fault, KFZ-Kiewa fault zone, IFZ-Indi fault zone.

- The absence of metamorphic hinterland, but localized high-tempe/low-pressure metamorphic regions.
- The absence of thrust slices or windows exposing Proterozoic basement.
- Large volumes of granite (up to 30% exposed area) where the distribution and ages of the granites do not fit simple orogenic models involving either A or B type subduction.
- Major fault zones in the turbidite-dominated part containing slices of oceanic crust associated with blueschist blocks in serpentinite- and mud-matrix mélangé.

21.4.2 Crustal Structure and Main Tectonic Elements

Eastern Australia (The Tasman Orogen) is made up of three north-south trending deformed belts (Delamerian, Lachlan/Thomson, and New England Orogens, Figure 21.4.1), which are distinguished by their lithofacies, tectonic settings, timing of orogenesis, and eventual consolidation to the Australian craton (Table 21.4.1). These represent three distinct tectonic settings: (1) deformed intracratonic rift (Delamerian Orogen), (2) deformed marginal turbidite fan system(s) in a backarc setting (Lachlan Orogen), (3) deformed arc-subduction complex belt (New England Orogen). The changing settings are part of a progressive eastwards younging of accretion along the evolving Australian continental margin, defined by their respective peak deformations of Late Cambrian–Early Ordovician, Late Ordovician–Silurian, and Permian–Triassic age (Table 21.4.1). Boundaries between the three belts are not exposed and generally they are covered by younger sequences. The inner belt (the Delamerian and

the western part of the Lachlan) shows pronounced curvature and structural conformity with the promontories and recesses in the old cratonic margin (the Tasman line; Figure 21.4.1). Outboard, the central and eastern belts of the Lachlan, and the New England belt, have more continuous trends that truncate the inner belt trends and thus show no relationship to the old cratonic margin.

Delamerian Orogen

The Delamerian fold belt (Orogen) is an arcuate, craton-verging thrust belt (Figure 21.4.2 and 21.4.3), with foreland-style folds and detachment-style thrusts (external zone) to the west, and a metamorphic hinterland (internal zone) to the east, characterized by polyphase deformation, amphibolite-grade metamorphism with local development of kyanite-sillimanite assemblages, and intrusion of syn- and posttectonic granites. During the Late Cambrian–Early Ordovician (locally called the Delamerian Orogeny) allochthonous sheets consisting of northwest-verging duplexes (deformed Cambrian Kanmantoo Group) were emplaced over the less deformed and metamorphosed shelf sequence (Adelaidean) of the external zone. High-temperature metamorphism formed at 300–500 MPa (~10–17 km depth) and is spatially and temporally confined to aureoles of synkinematic granites that are conformably aligned with the structural grain. Rapid unroofing (~10 km in approximately 20 m.y.) of the belt is suggested by juxtaposition of these high-grade rocks and their syntectonic granites (520–490 Ma) with undeformed, high-level silicic granites and volcanics intruded at 486 Ma. This provides a source for the extensive Ordovician turbidite sequences of the Lachlan Orogen to the east.

TABLE 21.4.1		OROGENS AND SUBPROVINCES OF THE TASMAN OROGENIC BELT			
Characteristic	Delamerian	Lachlan			New England
		Western	Central	Eastern	
Main plutonism	Late Cambrian	Late Devonian	Late Silurian	Late Carboniferous	Late Permian- Early Triassic
Tectonic vergence	W-directed thrusting	E-directed thrusting	Overall strike-slip with SE- directed thrusting	E-directed thrusting	W-directed thrusting
Terminal folding	Mid- Cambrian	Middle Devonian	Middle Silurian	Early Carboniferous	Mid-Permian
Main facies	Platform to deep water passive margin sequence	Quartz-rich turbidite sequence on oceanic crust	Quartz-rich turbidite Sequence on oceanic crust	Platform carbonates and clastics with rhyolites and dacitic tuffs	Volcanogenic clastic
Initial record	Basic volcanics	Cambrian basic volcanics	Tremadocian chert	Ordovician andesitic volcanics	Ordovician basic volcanics

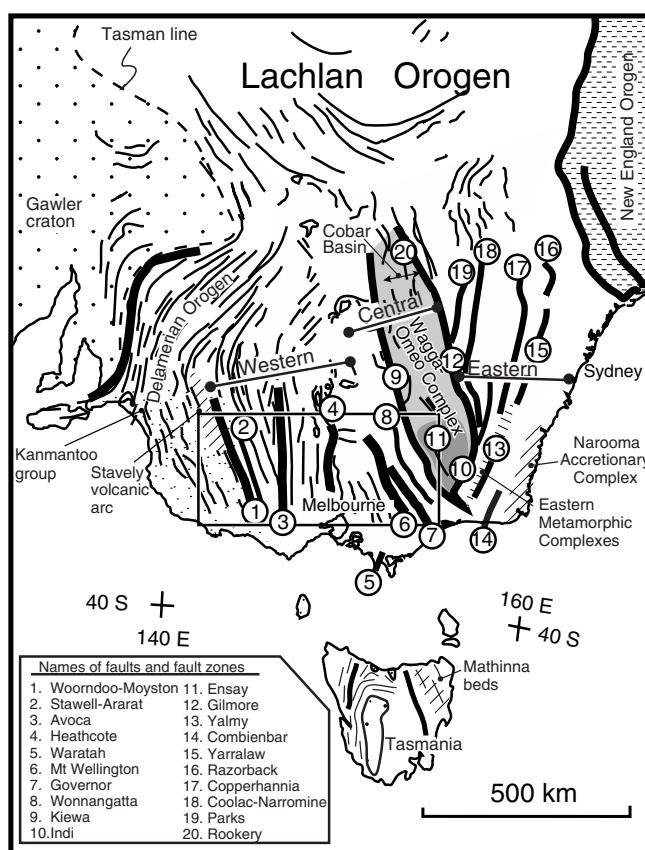


FIGURE 21.4.3 Structural trend map of the Lachlan Orogen and Tasman Orogen, combining aeromagnetic trend-lines and outcrop traces from regional maps and satellite images. The western, central, and eastern subprovinces are identified along with major faults [1–20].

The Delamerian Orogen was tectonically active from the Late Precambrian (~650–600 Ma) to the Early Ordovician (~500 Ma) and is part of the worldwide Pan-African orogenesis. It consists of a deformed Upper Proterozoic Adelaidean intracratonic rift sequence of marine to deltaic sandstones and shales, lagoonal evaporites, dolomites, and limestone, transgressed by lower Cambrian shelf sediments transitional into deep-water sandstones and mudstones. These units are progressively exposed in thrust slices as part of the craton-verging thrust system.

Lachlan Orogen

The Lachlan Orogen is a Middle Paleozoic fold belt with a 200-my history that occupies ~50% of the present outcrop of the Tasman Orogen (Figures 21.4.1 and 21.4.3). The major feature of the Lachlan fold belt is the similarity of sedimentary facies and overall structural style across this segment of the Tasman orogenic zone (Figure 21.4.2). Lower Paleozoic deep-water, quartz-rich turbidites, calc-alkaline volcanic rocks, and voluminous granitic plutons dominate the Lachlan Orogen. The turbidites overlie a mafic lower crust of oceanic affinity. They are laterally extensive over a present width of 800 km and have a current thickness upwards of 10 km. Large parts of the Lachlan Orogen represent accreted parts of a very large submarine sediment dispersal system associated with the Gondwana margin during the Early Paleozoic. This sediment

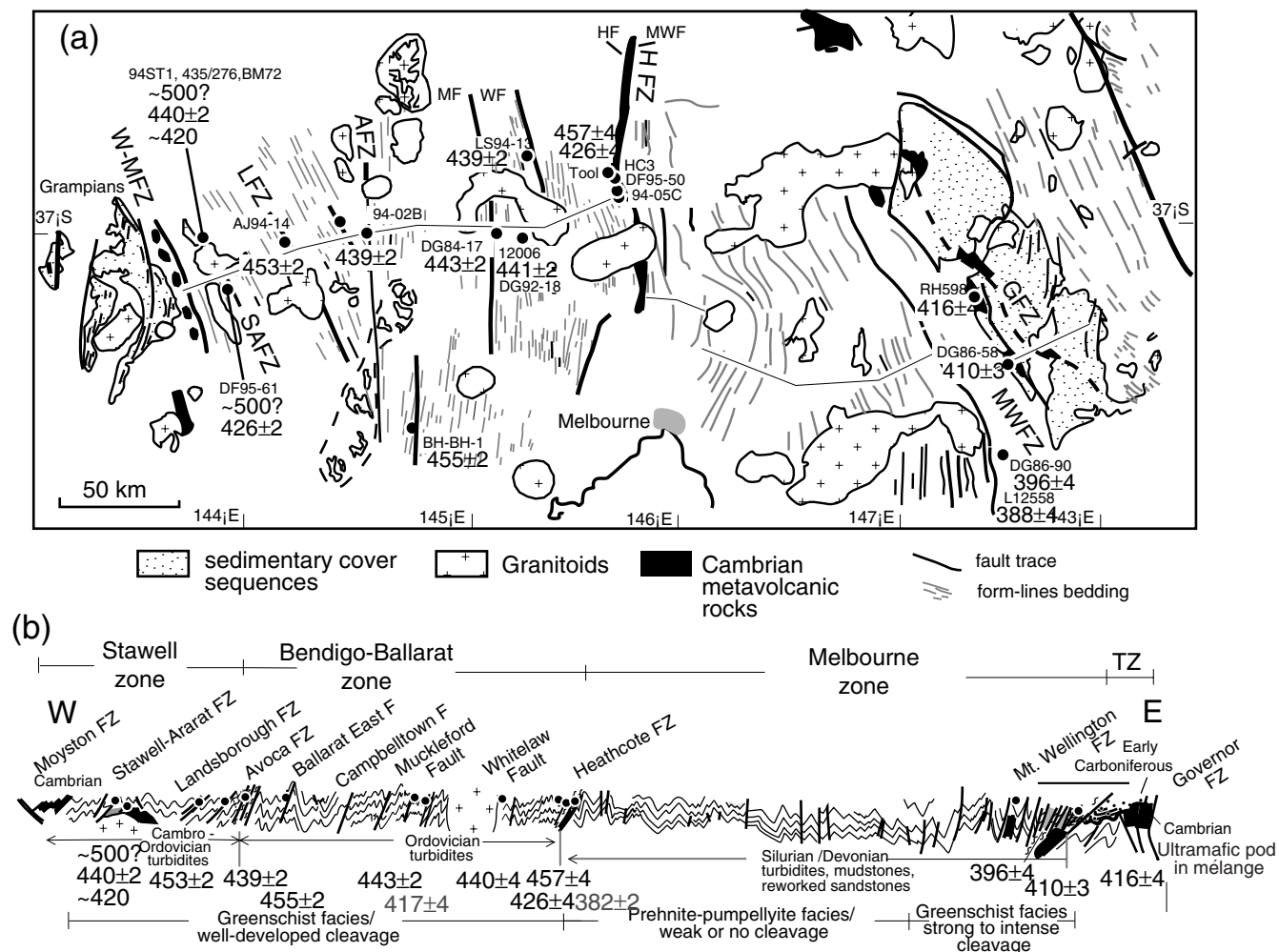


FIGURE 21.4.4 Structural trend map (a) and structural profile (b), with degree of cleavage development and grade of metamorphism of the western sub-province of the Lachlan Orogen incorporating the Stawell, Bendigo-Ballarot, and Melbourne structural zones. Faults are shown as heavy lines; abbreviations in (a) correspond to faults in (b). Dots show positions for $^{40}\text{Ar}/^{39}\text{Ar}$ ages that are given in Ma.

dispersal system must have been dimensionally comparable to the present-day Bengal fan in the Bay of Bengal. Within the turbidite succession, linear north-south trending, fault-bounded Cambrian metavolcanic belts, composed of boninite (high-Mg andesites), low-Ti andesite, and tholeiite of oceanic affinities, define the boundaries between different structural zones (Figures 21.4.2 and 21.4.3). The eastern part consists of shoshonitic (high-K) volcanics, mafic volcanoclastic rocks, and limestone, as well as quartz-rich turbidites and extensive black shale in the easternmost part.

Tight to open chevron folds (accommodating between 50% and 70% shortening), cut by predominantly west-dipping, high-angle reverse faults, are part of different thrust systems within the Lachlan Orogen (Figure 21.4.4). Chevron folds are upright and gently plunging but become inclined and poly-deformed

approaching major faults. Faults in the western part of the Lachlan fold belt are brittle faults, but they have high strain zones of varying widths that show the intense development of crenulation cleavages associated with variably but generally steeply plunging mesofolds and microfolds. Overprinting cleavages within these zones indicate complex fault movements in which early thrusting is followed by minor wrench movements. Detachments at the mid-crustal level occur at the base of the Ordovician and within the Cambrian successions in the western belt; deep crustal seismic profiling indicates a depth to detachment of approximately 15 km.

Metamorphism is greenschist facies or lower across the Lachlan Orogen, except in the shear zone-bounded Wagga-Omeo and several smaller metamorphic complexes that are part of the Eastern Metamorphic belt

(Figure 21.4.3), where high temperature–low pressure metamorphism is characterized by andalusite-sillimanite assemblages. Such assemblages are typical of thermal metamorphism, but here they occur on a regional scale. Peak metamorphic conditions in the Wagga-Omeo zone are $T \approx 700^\circ\text{C}$ and $P \approx 300\text{--}400$ MPa. Erosional unroofing of the metamorphic complex in the Middle to Late Silurian necessitates shallow overburden and high geothermal gradients on the order of $65^\circ\text{C}/\text{km}$. It is apparent that regional metamorphism and felsic magmatism throughout the orogen took place under very little cover, a scenario that suggests a shallow to mid-crustal heat input for melting.

Granites cover up to 36% of the exposed Lachlan Orogen. Regional aureole, contact aureole, and subvolcanic field associations, as well as sedimentary and igneous types based on geochemistry and/or mineralogy have been recognized. Most granites are posttectonic and are undeformed and have narrow (1–2-km wide) contact aureoles. Some of these are composed of subvolcanic granites associated with rhyolites, and ash flows of similar composition. The regional aureole types are less common and are associated with the high-temperature/low-pressure metamorphism, migmatites, and K feldspar-cordierite-andalusite-sillimanite gneisses. The shape distribution of the granites suggests three major granite provinces, which presumably reflect the mode and timing of emplacement and state of stress in the mid to lower crust. Elongate north-northwest to north-trending granites define the Wagga-Omeo metamorphic belt and the major part of the eastern Lachlan Orogen in New South Wales. Many of these granites are syntectonic and show the internal deformation and emplacement associated with deep-crustal shear zones. In the western Lachlan fold belt posttectonic granites of the central Victorian magmatic province, the largest granitic bodies, are east-west trending and have elongated form. The remaining granites are smaller and are more equant in shape. Spacing of the granitic bodies in Victoria fits a diapiric emplacement model with a source depth at 12–24 km, and possibly deeper, in a crust that was at least 35 km thick.

The Lachlan Orogen has undergone a complex history of amalgamation and deformation, in which there is an interplay of compressional and extensional events. Long-lived subduction in the Middle Paleozoic is envisaged along the Gondwana margin, but there is no evidence for major collision. Surface structures have been used to infer convergent margin deformation, and Ordovician volcanic rocks in New South Wales and relicts of blueschist metamorphism in fault zones in Victoria have been used to define the plate margin setting. As a consequence, the tectonic setting

and evolution of the Lachlan Orogen have been contentious. Significant advances, however, have been made in the last five to ten years due to (1) better resolution on the absolute timing and patterns of deformation (see next section), (2) different approaches to understanding the origin of the granitic plutons, (3) better understanding of the Ordovician arc in the east, (4) greater knowledge nature of the lower crust, and (5) a realization of the significance of the fault zones.

New England Orogen

The New England Orogen is the youngest and most easterly part of the Tasman belt (Figure 21.4.1). A collage of deformed and imbricated terranes (Figure 21.4.6a), it consists of largely Middle to Upper Paleozoic and Lower Mesozoic marine to terrestrial sedimentary and volcanic rocks, as well as strongly deformed flysch, argillite, chert, pillow basalts, ultramafic rocks, and serpentinites. The New England Orogen was tectonically active from the Late Devonian to the Middle Cretaceous (~95 Ma) and activity of this convergent margin involves arc, forearc, and accretionary complexes.

Widespread climactic Permian-Triassic deformation, involving west-directed thrusting, interleaving and imbrication of the arc magmatic belt (Connors-Auburn belt), forearc (Yarrol-Tamworth belt) and oceanic assemblages, including subduction complexes (Wandilla-Gwydir belt) and ophiolite (Gympie belt), consolidated the terranes into Australia and caused the development of a Permo-Triassic foreland basin (Sydney-Bowen Basin). Complex outboard subduction assemblages show a strong thrust-related fabric, polyphase deformation, and greenschist to amphibolite facies metamorphism.

21.4.3 Timing of Deformation and Regional Events

The timing of orogenic events in the Lachlan Orogen has been broadly defined by the ages of strata over regional unconformities and by the age of stitching plutons. More recently $^{40}\text{Ar}/^{39}\text{Ar}$ data from metamorphic white mica in the low-grade metasedimentary rocks and associated quartz veins give precise estimates on the timing of cleavage formation and regional deformation events. This is because, in these fine-grained strongly cleaved rocks, the only significant K-bearing phase after metamorphism is metamorphic white mica that typically retains argon at temperatures greater than those under which it grew. Mica growth below the closure temperature provides a definitive

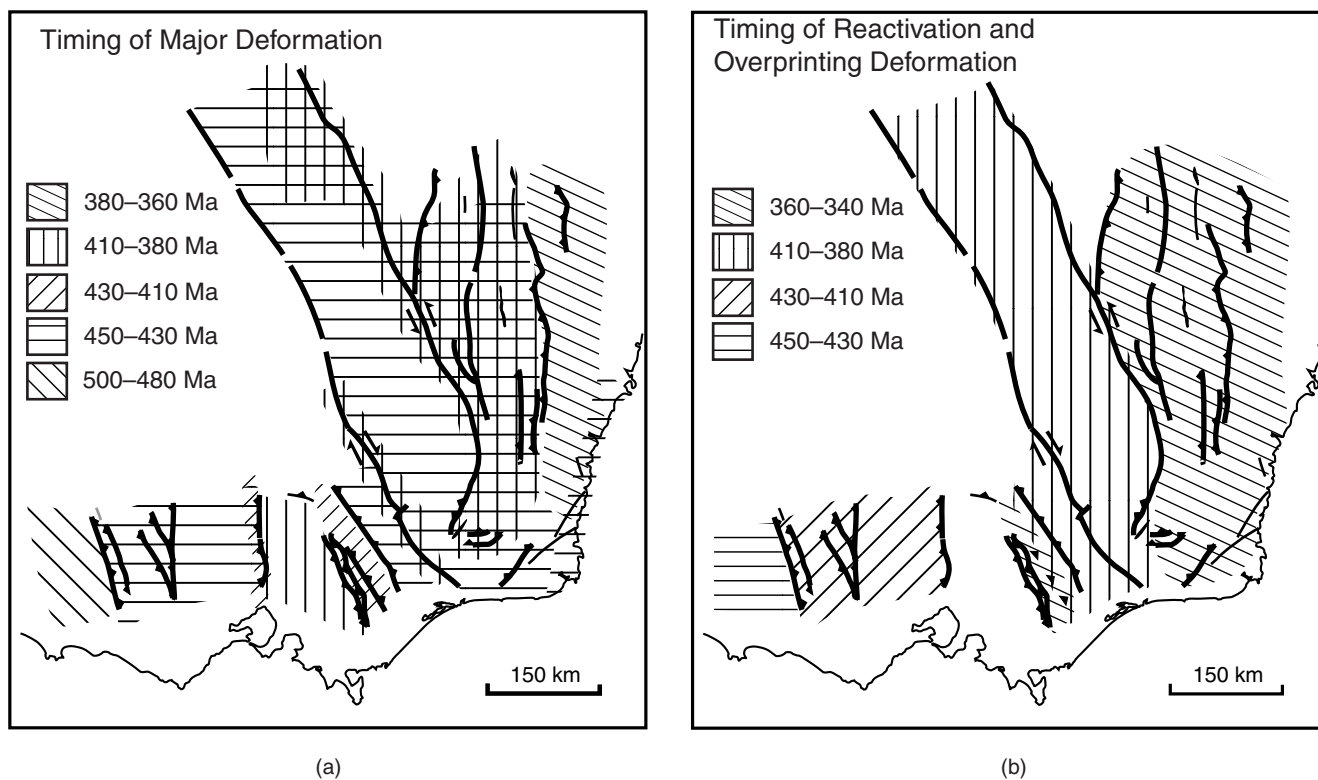


FIGURE 21.4.5 Maps of the Lachlan Orogen showing timing of deformation events and fault reactivation, based on $^{40}\text{Ar}/^{39}\text{Ar}$ geochronology and other geologic constraints.

method for dating the cleavage-forming part of the deformation, and the timing of regional metamorphism. Fine-grained metamorphic phengites close to argon loss at about 350°C , so that at very low greenschist and prehnite-pumpellyite facies metamorphic conditions, they grow at or below their closure temperatures. $^{40}\text{Ar}/^{39}\text{Ar}$ ratios for rocks in the high-grade metamorphic complexes give the timing of exhumation, so, wherever possible, deformation in these areas is dated by U-Pb zircon data.

The $^{40}\text{Ar}/^{39}\text{Ar}$ geochronologic and thermochronologic data, interpreted along with other geologic data, allow us to define when specific regions within the Lachlan Orogen first underwent significant deformation, metamorphism, faulting, and reactivation (Figure 21.4.5). Deformation in the Lachlan Orogen was initiated between ~ 455 and 430 Ma in three areas: the western subprovince, where it migrated eastward; the central subprovince, where it migrated to the southwest; and the eastern subprovince in the Narooma accretionary complex (Figure 21.4.3). The western subprovince is characterized by major deformation in the Stawell and Bendigo-Ballarat zones between ~ 455 and 440 Ma and fault reactivation at ~ 430 – 410 Ma. The eastern bounding fault of the western Lachlan, the Mount Wellington fault zone (Figure 21.4.3), was

active between 410 and 385 Ma and reactivated during Carboniferous time.

The central subprovince (Figure 21.4.3) underwent major deformation in the high-grade metamorphic complex between 440 and 430 Ma, and was exhumed between ~ 410 and 400 Ma, as shown by mica dating from the shear zones bounding the complex. To the west, in low-grade metasedimentary turbidites (Figure 21.4.2), deformation began at ~ 440 – 430 Ma and migrated southwestward until ~ 410 – 416 Ma. Later deformation took place when the eastern subprovince collided with the western subprovince at ~ 400 – 380 Ma, and again during the Carboniferous. The oldest recorded deformation in the eastern subprovince (Figure 21.4.3) took place in the Narooma complex ~ 455 – 445 Ma, when it was outboard of and separated from the rest of present eastern subprovince. The inland parts of the eastern subprovince are dominated by contractional deformation that occurred 400 – 380 Ma and there was additional deformation 380 – 360 Ma in the central and northeastern region. These younger episodes overprint the earlier fabrics such as those in the Narooma complex. The Silurian extensional event predated this contractional deformation phase. Although very widespread, intense Carboniferous deformation is almost unique to the north-

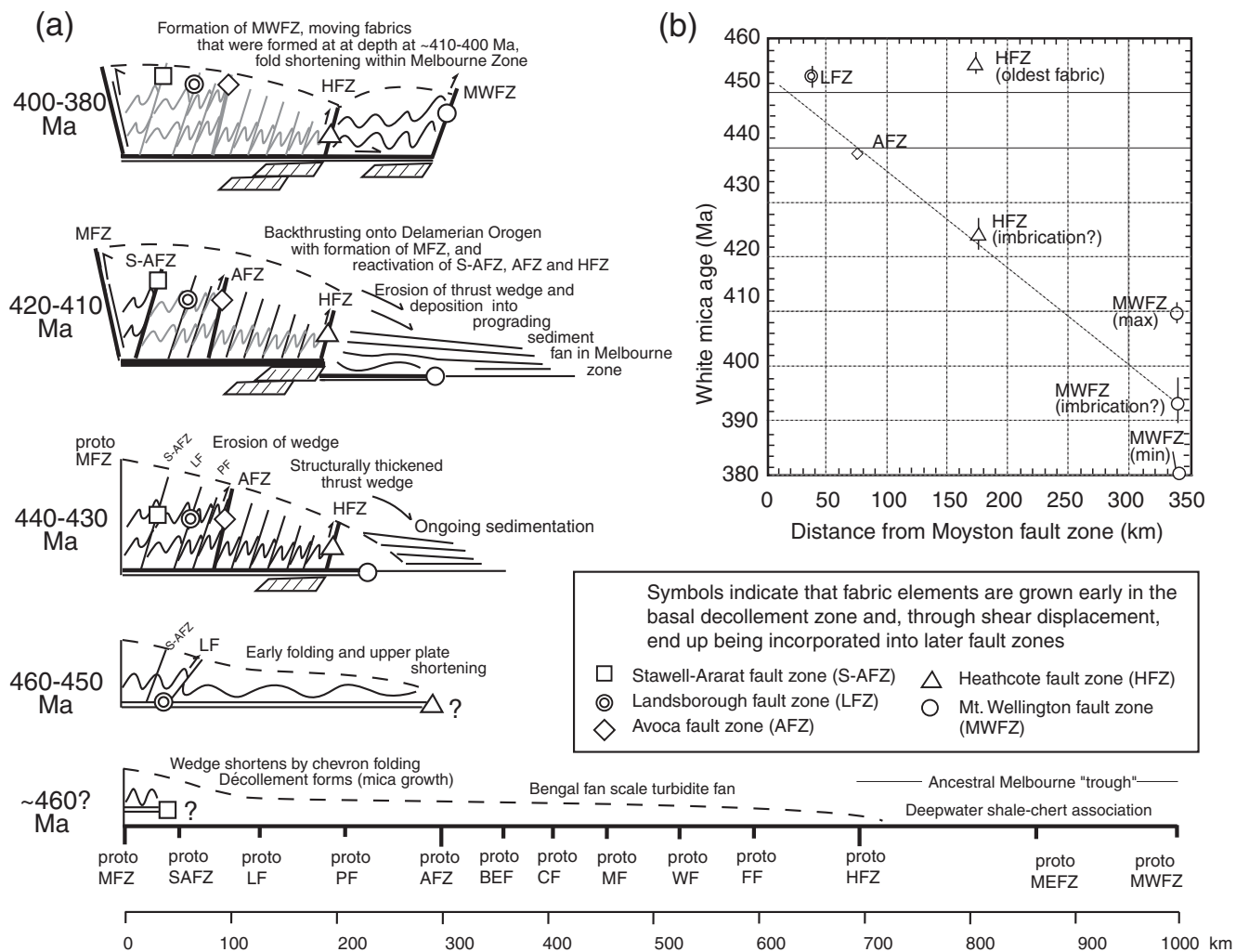


FIGURE 21.4.6 Progressive deformation sequence for the western Lachlan Orogen based on the observed thrust-belt geometry and the requirement of underthrusting from the east. There is an implied diachronous progression of chevron folding, imbrication, and unroofing from a deep level décollement. A consequence of the model is that shortening has to be achieved above the basal fault to attain critical taper prior to movement along it. This means that some mica ages within thrust sheets may be older or at least coeval with the mica ages from the basal fault zone splays. The $Ar^{40/39}Ar$ data suggest that folding, quartz veining, cleavage development, and faulting progressed eastwards from Middle Ordovician (~455 Ma) through the Middle Devonian (~390–380 Ma). Fault zones record multiple ages due to multiple episodes of reactivation, crenulation cleavage, and fabric transposition. (b) Fault propagation shown as a graph of white mica age [Ma] versus distance from the Moyston fault zone [i.e., the westernmost part of the Lachlan Orogen]. This is based on the youngest significant $Ar^{40/39}Ar$ ages from the major fault zones (listed on the figure) of the western Lachlan. These data require diachronous but not necessarily continuous deformation. If it is assumed that deformation was continuous over this interval, then the time-averaged fault propagation rate is ~6 mm/y. Abbreviations:

ern part of the Lachlan Orogen in the eastern sub-province. Carboniferous deformation partly reflects the progressive eastward accretion of the Tasmanides and is probably related to amalgamation of the New England Orogen. The Carboniferous could even include the rapid movement of Australia toward the south pole, a process that may have also caused the Alice Springs Orogeny in central Australia.

In the past, a framework of six orogenic events was proposed for the Lachlan Orogen during the Paleozoic. It now appears that some of these events are

localized and strongly time-transgressive. Because of the complex and localized pattern of deformation during the Ordovician, Silurian, and Devonian we have preferred to refer to the whole interval as the Lachlan Orogeny. Based on the present data it has been argued that two major events still dominate the Middle Paleozoic—one at ~440–430 Ma and one at ~390–380 Ma. However, because significant tectonic activity in terms of strike-slip faulting and plutonism continued between these “events” we prefer to use the broader framework.

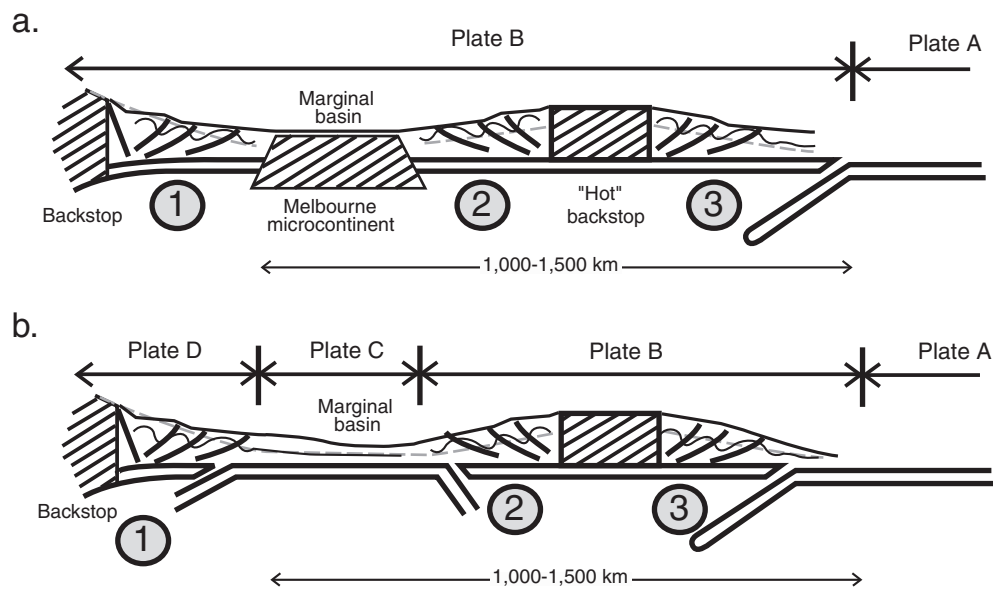


FIGURE 21.4.7 Tectonic interpretation of simultaneous, eastward and westward propagating and migrating deformation fronts in the western, central, and eastern parts of the Lachlan Orogen. Deformation is due to underthrusting of a sediment wedge between three proposed subduction systems that were from 1500 to 2000 km apart in the Late Ordovician–Early Silurian.

21.4.4 Mechanics of Deformation in Accretionary Orogens

Turbidite-dominated, accretionary orogens, such as the Lachlan Orogen of eastern Australia and those in central Asia and some Pan African belts, differ from classical orogenic belts such as the Alps, Appalachians, and North American Cordillera. The latter were constructed partly of shelf sequences developed along margins of moderately thick (~30–40 km) continents, whereas the former are characterized by monotonous, commonly chevron-folded turbidites that overlie oceanic crust and, in places, thin, attenuated continental crust.

Faults in the low-grade turbidite sequences of turbidite-dominated accretionary orogens record the kinematic evolution of this style of orogen. These fault zones are characterized by higher than average strain and intense mica fabrics, transposition foliation and isoclinal folds, poly-deformation with overprinting crenulation cleavages, and steeply to moderately plunging meso- and microfolds. They have a different character compared to the brittle-ductile fault zones of classic foreland fold-and-thrust belts such as are found in the Appalachians and the Canadian Rocky Moun-

tains. Multiple cleavages and transposition layering record a progressive shear-related deformation history. An intense mica fabric evolves initially during shortening of the overlying sedimentary wedge, but this fabric is progressively modified during rotation and emplacement to higher structural levels along the steep parts of inferred listric faults. The deformed wedge outside the fault zones generally undergoes one phase of deformation, shown by a weak to moderately developed slaty cleavage, which is parallel to the axial surface of upright, subhorizontally plunging chevron-folds. In the Lachlan Orogen we have interpreted the structural evolution constrained by $^{40}\text{Ar}/^{39}\text{Ar}$ dating to consist of progressive deformation associated with simultaneous, eastward propagating and migrating deformation fronts in both the western and the eastern parts of the fold belt (Figure 21.4.6). These deformation fronts are related to accretionary style deformation at the leading edges of overriding plates, in an inferred southwest Pacific-type subduction setting from the Late Ordovician to the Middle Devonian, along the former Gondwana margin (Figure 21.4.7). The fault zones effectively accommodate and preserve movements within structurally thickening, migrating, and prograding sediment wedges.

ADDITIONAL READING

- Collins, W. J., 1996. Lachlan fold belt granitoids—products of three-component mixing. *Transactions of the Royal Society of Edinburgh, Earth Sciences*, 87:171–181.
- Collins, W. J., 1998. Evaluation of petrogenetic models for Lachlan fold belt granitoids: implications for crustal architecture and tectonic models. *Australian Journal of Earth Sciences*, 45, 483–500.
- Coney, P. J., Edwards, A., Hine, R., Morrison F., Windrum, D., 1990. The regional tectonics of the Tasman orogenic system, eastern Australia. *Journal of Structural Geology*, 125, 19–43.
- Fergusson, C. L., Coney, P. J., 1992. Convergence and intraplate deformation in the Lachlan fold belt of southeastern Australia. *Tectonophysics*, 214, 417–39.
- Foster, D. A., Gray D. R., 2000. The structure and evolution of the Lachlan fold belt (Orogen) of eastern Australia. *Annual Reviews of Earth and Planetary Sciences*, 28, 47–80.
- Foster, D. A., Gray, D. R., Bucher, M., 1999. Chronology of deformation within the turbidite-dominated Lachlan orogen: implications for the tectonic evolution of eastern Australia and Gondwana. *Tectonics*, 18, 452–485.
- Gray, D. R., 1997. Tectonics of the southeastern Australian Lachlan fold belt: structural and thermal aspects. In Burg, J. P., Ford, M., eds., *Orogeny through time, Geological Society Special Publication*, 121, 149–177.
- Gray, D. R., Foster, D. A., 1997. Orogenic concepts—application and definition: Lachlan fold belt, eastern Australia. *American Journal of Science* 297, 859–891.
- Gray, D. R., Foster, D. A., 1998. Character and kinematics of faults within the turbidite-dominated Lachlan orogen: Implications for the tectonic evolution of eastern Australia. *Journal Structural Geology* 20, 1691–1720
- Gray, D. R., Foster, D. A., Gray C., Cull J., Gibson, G., 1998. Lithospheric structure of the southeast Australian Lachlan fold belt along the Victorian Global Geoscience Transect. *International Geology Review* 40, 1088–1117.
- Spaggiari, C. V., Gray, D. R., and Foster, D. A., 2002. Blueschist metamorphism during accretion in the Lachlan Orogen, southeastern Australia. *Journal of Metamorphic Geology*, 20, 711–726.
- Spaggiari, C. V., Gray, D. R., Foster, D. A., and Fanning, C. M., 2002. Occurrence and significance of blueschist in the southern Lachlan Orogen. *Australian Journal of Earth Sciences*, 49, 255–269.